Plant Science 338 (2024) 111896

Contents lists available at ScienceDirect

Plant Science

journal homepage: www.elsevier.com/locate/plantsci

Maize (*Zea mays* L.) root exudation profiles change in quality and quantity during plant development – A field study

Michael Santangeli [a,b,1], Teresa Steininger-Mairinger [b,2], Doris Vetterlein [c,d,3], Stephan Hann [b,4], Eva Oburger [a,5,*]

[a] University of Natural Resources and Life Sciences, Vienna, Department of Forest and Soil Science, Institute of Soil Research, 3430 Tulln an der Donau, Austria
[b] University of Natural Resources and Life Sciences, Vienna, Department of Chemistry, Institute of Analytical Chemistry, 1190 Vienna, Austria
[c] Department of Soil System Science, UFZ, 06120 Halle/Saale, Germany
[d] Institute of Agricultural and Nutritional Sciences, Martin Luther University Halle-Wittenberg, 06120 Halle/Saale, Germany

ARTICLE INFO

Keywords:
Rhizosphere
Root hairs
Carbon flux
Rhizodeposition
Root traits
Soil texture
LC-QTOFMS
Non-targeted metabolomics

ABSTRACT

Deciphering root exudate composition of soil-grown plants is considered a crucial step to better understand plant–soil–microbe interactions affecting plant growth performance. In this study, two genotypes of *Zea mays* L. (WT, *rth3*) differing in root hair elongation were grown in the field in two substrates (sand, loam) in custom-made, perforated columns inserted into the field plots. Root exudates were collected at different plant developmental stages (BBCH 14, 19, 59, 83) using a soil-hydroponic-hybrid exudation sampling approach. Exudates were characterized by LC-MS based non-targeted metabolomics, as well as by photometric assays targeting total dissolved organic carbon, soluble carbohydrates, proteins, amino acids, and phenolics. Results showed that plant developmental stage was the main driver shaping both the composition and quantity of exuded compounds. Carbon (C) exudation per plant increased with increasing biomass production over time, while C exudation rate per cm^2 root surface area h^{-1} decreased with plant maturity. Furthermore, exudation rates were higher in the substrate with lower nutrient mobility (i.e., loam). Surprisingly, we observed higher exudation rates in the root hairless *rth3* mutant compared to the root hair-forming WT sibling, though exudate metabolite composition remained similar. Our results highlight the impact of plant developmental stage on the plant–soil–microbe interplay.

1. Introduction

In view of the continuously growing food demand, improving knowledge of the plant-soil-microbe interactions is fundamental to enhancing agricultural production and adaptation to abiotic stresses in a sustainable way (Galindo-Castañeda et al. 2022; Inbaraj, 2021; Oburger et al. 2022a). Root exudates play a key role in the cross-talk between plants, microbiomes, and soil which in turn also affects plant growth performance. Consequently, in-depth knowledge of root exudation dynamics will improve our understanding of below-ground processes and their interactions and feedback loops. Root exudates comprise a complex mixture of metabolites continuously produced by plants and are released by roots into the soil (Oburger and Jones, 2018). By fuelling rhizosphere processes, including microbiome composition and activity, root exudates also directly have an impact on carbon (C) and nutrient cycling, greenhouse gas emissions as well as soil structure formation (Badri and

Abbreviations: QTOFMS, Quadrupole time of flight mass spectrometry; LC, Liquid chromatography; MS, Mass spectrometry; HILIC, Hydrophilic interaction liquid chromatography; BBCH, Biologische Bundesanstalt, Bundessortenamt und Chemische Industrie; RD, Root average diameter; RSA, Root surface area; RL, Root length; RLD, Root length density; OPLS-DA, Orthogonal projection to latent structures discriminant analysis; DOC, Dissolved organic carbon; C, Carbon; VIP, Variable importance of projection.

* Corresponding author.
E-mail address: eva.oburger@boku.ac.at (E. Oburger).
[1] 0000-0002-0552-7173
[2] 0000-0001-7809-1529
[3] 0000-0003-2020-3262
[4] 0000-0001-5045-7293
[5] 0000-0003-3213-2588

https://doi.org/10.1016/j.plantsci.2023.111896
Received 14 July 2023; Received in revised form 2 October 2023; Accepted 10 October 2023
Available online 12 October 2023

Vivanco, 2009; Philippot et al. 2009). Root exuded substances are generally divided into two classes of compounds: low-molecular-weight compounds (LMW) and high-molecular-weight compounds (HMW) (Badri and Vivanco, 2009; Oburger and Jones, 2018). The former includes primary and secondary metabolites such as amino acids, organic acids, sugars, and phenolics, whereas proteins, mucilage, and polysaccharides belong to the latter (Baetz and Martinoia, 2014; Bais et al. 2006). Due to their physical and biochemical characteristics, a large number of metabolites, especially secondary, were reported to trigger a cascade of interactions with soil microbes and/or neighbouring plants, with some protecting against and others attracting pathogens and herbivores (Badri and Vivanco, 2009; Lambers et al. 2009; Millet et al. 2010; Oburger et al. 2022a; Rudrappa et al., 2008; Weston and Mathesius, 2014). Furthermore, type and amount of substances secreted as root exudates were found to vary depending on biotic and abiotic factors including water and nutrient availability, as well as metal toxicity (Canarini et al. 2016; Carvalhais et al. 2011; Preece and Peñuelas 2016; Wang et al. 2018), and soil microbial community composition (Jones et al. 2004; Leyval and Berthelin, 1993; Meier et al. 2013). Previous studies have also demonstrated that exudation profiles change with plant development, revealing contrasting regulation for specific compound classes in different species, with some of the observed differences being potentially related to the different methodological approaches applied (e.g., Chaparro et al. 2013; De-la-Peña et al. 2010; Zhao et al. 2021). However, due to experimental constraints, a rather limited number of studies investigated changes in exudation patterns across plant developmental stages in crop species (Aulakh et al. 2001; Gransee and Wittenmayer, 2000; Zhalnina et al. 2018). Nevertheless, evidence so far suggests that plants adjust root exudation profiles in response to changing physiological and metabolic needs at different growth stages. For instance, young plants were found to invest more C in root growth and root exudation (Pantigoso et al. 2020), while at maturity, as their nutrient requirement stabilizes, plants were observed to release more allelopathic or defence related compounds to suppress competing plants or potential pathogens (Chaparro et al. 2014; Hu et al. 2018). This change in exudation depending on developmental stage as well as biotic and abiotic factors may therefore pose a relevant factor in the plant's resilience to environmental stresses.

Next to plant development, it has been observed that root exudation is also influenced by root traits such as root diameter, root architecture, and the presence of root hairs. This indicates that tissue (growth) dependent carbon (C) belowground allocation affects root exudation dynamics. Furthermore, these root traits play a crucial role in determining the plant's efficiency in acquiring resources (Guyonnet et al. 2018; Williams et al. 2022). Among root traits, root hairs have been reported to play a significant role in nutrient and water uptake (Bienert et al. 2021; Cai and Ahmed, 2022; Jungk, 2001) and rhizosheath formation (Burak et al. 2021), further facilitating beneficial interactions with soil microorganisms (Rongsawat et al. 2021). However, there is still limited knowledge about the contribution of root hairs to root exudation and contrasting reports can be found for agriculturally relevant crop species. For instance, previous studies have indicated that root hairs increase exudation and rhizosphere extent in maize and barley (*Hordeum vulgare*) (Holz et al. 2017; Ma et al. 2021). However, in a recent study on *Zea mays* L., Lohse et al. (2023) observed a higher C exudation rate in the *rth3* hairless mutant compared to the respective root hair forming WT. Additionally, Bilyera et al. (2022), applied different chemical imaging techniques *in situ* in root windows installed in the same field experiment as the present study and did not observe a clear effect of maize root hairs on rhizosphere pH and phosphatase activity extent.

Non-targeted metabolomics allows for a comprehensive and simultaneous (i.e., single run) analysis of small molecules spanning a wide physicochemical range (Fiehn, 2002). Several recent studies applied non-targeted metabolomic analysis to investigate root exudation and rhizosphere-related processes (Lohse et al. 2023; Miller et al. 2019; Mönchgesang et al. 2016; Pétriacq et al. 2017; Wang et al. 2019). However, the potential of metabolomics to investigate exudate driven processes can only be exploited when combined with carefully selected experimental growth and sampling conditions (Oburger and Jones, 2018; van Dam and Bouwmeester, 2016). Despite the increasing awareness of the ecological relevance of soil-based studies (Oburger and Jones, 2018; Oburger et al. 2022b), only a limited number of exudation studies have been carried out under field conditions and/or across plant developmental stages (e.g., Aulakh et al. 2001; Chaparro et al. 2013; Neumann et al. 2014; Weinhold et al. 2022). Sampling root exudates from soil grown plants is challenging as exuded metabolites strongly interact with the soil matrix (sorption) and are exposed to rapid microbial decomposition. Hydroponic growth conditions, on the other hand, are not representative for natural soil environments but facilitate exudate collection (Oburger and Jones, 2018). A possible compromise to collect root exudates in conditions that reflect natural soil growth is the soil-hydroponic-hybrid exudation sampling. This approach allows plants to grow in soil, while exudates are sampled hydroponically for a short period of time after careful root washing process (Oburger et al. 2014; Oburger and Jones, 2018). Consequently, the soil-hydroponic-hybrid setup is also applicable to field grown plants.

To improve our understanding on root exudation dynamics of agronomically relevant crop species like maize, this study aimed to reveal changes in root exudation patterns of two field grown maize lines (*Zea mays* (WT and root hair formation defective mutant *rth3*) at four different plant development stages (BBCH 14, 19, 59, 83) ranging from the vegetative to the ripening phase. Additionally, growing our maize lines in two substrates (loam (L), sand (S)) differing in soil texture and nutrient mobility enabled us to investigate the impact of plant genotype (i.e., the presence (WT) or absence (*rth3*) of root hairs) and substrate on maize root exudation patterns. As plants must balance their C allocation strategies to acquire nutrients and sustain their growth, especially during the vegetative growth phase, we expected exudation rates to be higher for juvenile plants (hypothesis 1). Furthermore, we hypothesized that exudation will be higher in substrates with lower nutrient mobility (i.e., loam) as plants are likely to adapt their nutrient acquisition strategies depending on the growth substrate (hypothesis 2). Despite the contrasting reports in the literature, we expected the presence of root hairs (WT) to increase root exudation rates due to the enhanced root surface area (hypothesis 3). Combining a (field) soil-based exudation sampling approach with non-targeted metabolomics analyses allowed us to acquire genotype, substrate, and growth stage specific resolved information about the metabolite patterns released by maize under field conditions.

2. Material and methods

2.1. Chemicals

All solvents and reagents used in this study were analytical grade or equivalent and acquired from Sigma Aldrich (Vienna, Austria), unless otherwise stated. LC solvents were LC-MS grade, and LC-MS water (MQW) was prepared using Milli-Q® IQ 7000 Ultrapure Lab Water System (Darmstadt, Germany) combined with a Milli-Q LC-Pak® Polisher.

2.2. Experimental design

The field experiment was conducted at the research station of Bad Lauchstädt, Germany (N 51.390424, E 11.875933) in 2019. A detailed description of the experimental field site and experimental setup can be found in Vetterlein et al. (2021). Briefly, two maize genotypes (*Zea mays* L. wildtype (B73) (WT) and the corresponding root hair defective mutant (*rth3*) (Wen and Schnable, 1994)) were grown in two soil substrates with varying textures. The experimental design followed a two-factorial randomized block design, with six plot replicates per

treatment (Fig. 1a). Treatments were defined by the combination of the two experimental factors, namely, loam-wild type (L-WT), loam-*rth3* (L-*rth3*), sand-wild type (S-WT), and sand-*rth3* (S-*rth3*). The *rth3* mutation encodes a COBRA-like protein that is responsible for cellulose assembly in the cell wall. It shows typical initiation but disrupted hair elongation, that did not cause any noticeable changes in the shoot phenotype, though under field condition its yield was reduced by 20–40% compared to the WT (Hochholdinger et al. 2008; Vetterlein et al. 2022). The soils used were a loam (L) substrate (Haplic Phaeozem) and a mixture of 16.7% loam with 83.3% quartz sand, from here on referred to as sand (S). Substrates were mixed to provide a source C_{org} to S, and to establish a similar initial microbiome composition across the substrates. Detailed information about the characteristics of both substrates were already described in Vetterlein et al. (2021).

Custom-made, perforated soil columns were designed and built to allow the excavation of one individual plant with an intact, undamaged root system from the field plots. Soil columns were made from coarsely perforated PE tubes (Fig. 1b) (diameter 20 cm, height 30 and 60 cm, with 5 cm wide, drilled holes) that were cut in two halves and screwed together through connectors and a PVC bottom plate (Fig. 1b) to facilitate installation and soil column retrieval. A nylon belt (5 cm width) was fixed at the bottom plate with both loose ends reaching the top of the column to help lift the soil columns. A nylon mesh (30 μm, SEAFAR Nitex, Heiden, Switzerland) was fixed on the inside of each soil column allowing the exchange/passage of water, solutes, and microorganisms but restricting root growth beyond the mesh barrier. Soil column height differed depending on plant growth stage, defined according to the BBCH scale from Bleiholder et al. (2001). Sampling points included: BBCH 14 (four leaves unfolded), BBCH 19 (nine or more leaves unfolded, exponential growth phase) BBCH 59 (end of tassel emergence, transition from vegetative to generative growth) and BBCH 83 (early dough, ripening phase) (Vetterlein et al. 2021), corresponding to four different plant phenological characteristics. Shorter columns (30 cm) were used for BBCH 14 and 19, while longer ones (60 cm height) were used for BBCH 59 and 83. In April 2019, before maize planting, soil columns were installed at the field site. Columns were inserted in individual plots and filled with the corresponding plot substrate, leading to 9425 cm^3 of soil volume available for plant growth for the short columns (30 cm height, BBCH 14 and BBCH 19) and 18850 cm^3 for the long columns (60 cm height, BBCH 59 and BBCH 83). The bulk density of the columns was 1.43 g/cm^3 for the loam and 1.65 g/cm^3 for the sand plots. Due to the destructive nature of this approach and the limited plot size, the number of columns had to be limited to four per plot and four replicates per treatment instead of six. Four soil columns, one for each

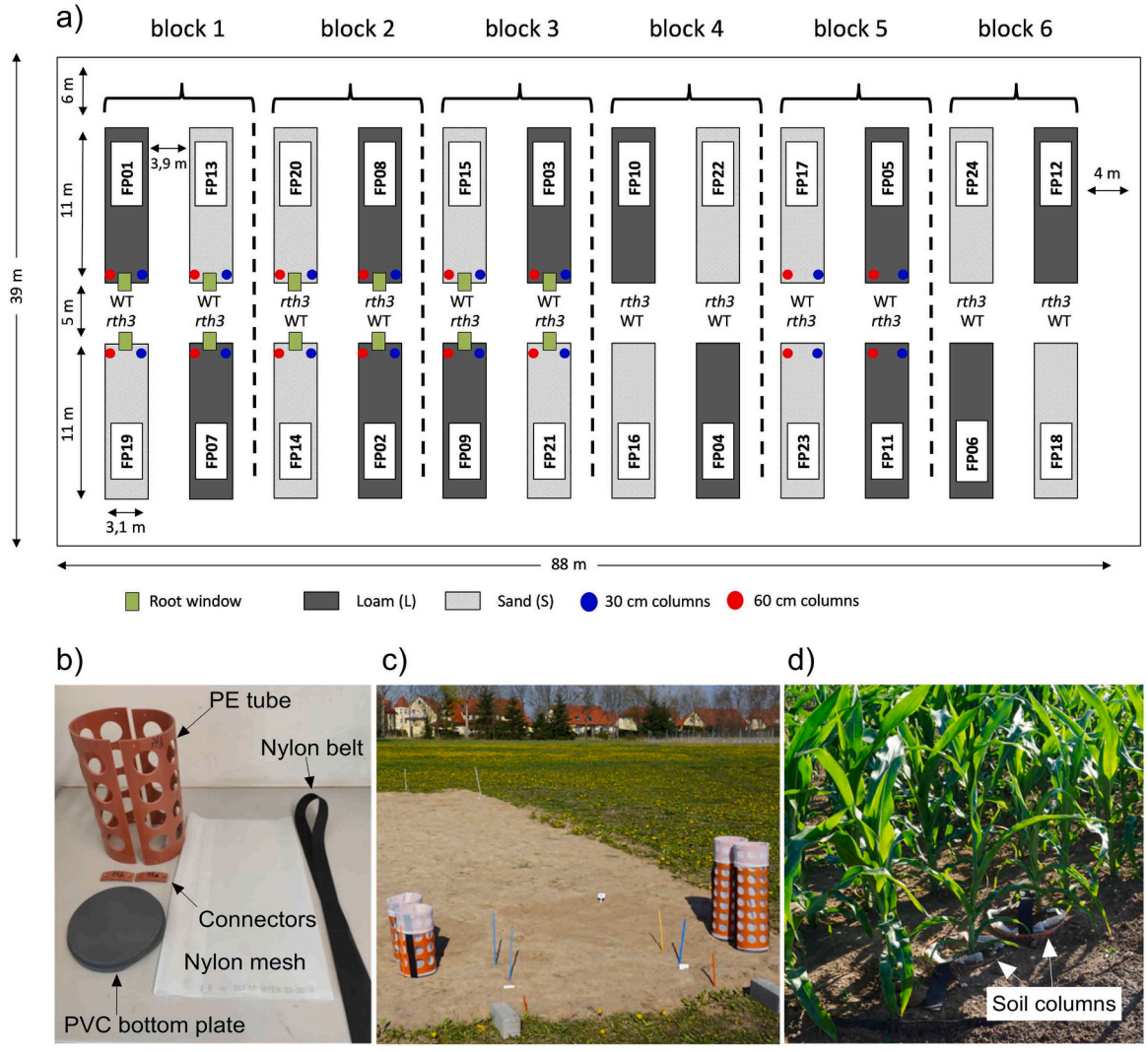

Fig. 1. (a) Soil plot experiment sketch with the relative position of soil columns within the field plots (FP) and root windows (Bilyera et al. 2022). Each block represents a replicate of the treatments (i.e., loam-wild type (L-WT), loam-root hair defective mutant (L-*rth3*), sand-wild type (S-WT), and sand-root hair defective mutant (S-*rth3*)) (Adapted from Vetterlein et al. (2021)). (b) Disassembled 30 cm soil column. (c) Assembled soil columns before installation. (d) Soil columns with maize plants installed in the field plots (BBCH 19; L-WT).

growth stage, were set up in four replicate plots for each treatment, for a total of 64 soil columns. The position of soil columns in the field plots is shown in Fig. 1a. Maize plants were sown on the 24th of April 2019 at a depth of 5 cm. One individual maize seed was planted in the middle of the soil column for BBCH 19, 59, 83, whereas, to have enough root biomass in the first growth stage, two maize seeds were planted in the BBCH 14 columns.

2.3. Root exudation sampling

To investigate the changes in root exudation of the two maize genotypes over the whole vegetation period, soil columns with intact maize plants were excavated at BBCH 14, 19, 59 and 83. Root exudates were sampled using a soil-hydroponic-hybrid approach (Oburger et al. 2014; Oburger and Jones, 2018), consisting in soil-grown plant, careful root washing and hydroponic exudation sampling. After removing soil columns from the field plot, columns and the nylon mesh were opened (Fig. S1a) and soil was carefully removed from roots by gentle rinsing with tap water for about 30 min (Fig. S1b, c). After the complete removal of soil particles, plants were soaked three times in fresh deionized (DI) water for five minutes each for osmotic adjustment and to capture metabolites released upon root damage. Thereafter, root exudates were collected in 0.5, 1, 4.5, and 7.5 L of sampling solution in polypropylene buckets for BBCH 14, 19, 59, and 83 respectively, first in DI water for one hour followed by a two hours sampling in the corresponding sampling volumes of MQW containing 0.01 g L^{-1} Micropur (MP) classic (Katadyn®, Switzerland) as microbial inhibitor agent (Oburger et al. 2014). The 0.01 g L^{-1} MP sampling solution allowed us to collect exudates unaltered by microbial decomposition during the sampling procedure as MP is known to inhibit microbial activity. The first exudation sampling period (1 h) in DI water without sterilizing agent was carried out to collect exudate solutions suitable for studying the effect of exudates on the soil microbiome and soil structure *ex situ* (not addressed here). Root exudates were sampled under ambient conditions with sampling buckets being covered with aluminium foil and green leaves from other plants to shield roots from sunlight and prevent light reflection from the aluminium foil surface. Detailed information about sampling volumes, timeline, Photosynthetically Active Radiation (PAR), and sampling duration are listed in Table S2.

At the end of the sampling period, roots were removed from the sampling solution and exudate solutions were filtered (0.2 μm, Cellulose acetate OE 66, Whatman, UK) to remove all root debris allowing us to capture the soluble exudate fraction only. The filtered exudates were split up in several aliquots, frozen at − 20 °C for 72 h, transported in dry ice and subsequently stored at − 80 °C until analysis.

2.4. Plant growth parameters and root traits

An aliquot of the fresh root system was taken, weighed, and stored in 1:1 water:ethanol (*v/v*) at 4 °C until analysis for morphological root system parameters. The remaining root aliquot and the shoot biomass were determined after 72 h of oven drying at 60 °C. Root aliquots stored in ethanol:water were scanned at 600 dpi with a flatbed scanner (EPSON Perfection V700) and the obtained images were analyzed with WinRHIZO Pro™ (Version 2007d, Regent Instruments, Canada). Total root length (RL), root surface area (RSA), root volume (RV), and root diameter (RD), were obtained by extrapolating the values of the WinRHIZO aliquot to the whole root system (calculated as dry mass of WinRHIZO aliquot + remaining roots biomass). Root to shoot ratio (R:S) was calculated dividing the root dry biomass per shoot dry biomass for each individual plant. Root traits were calculated as follows: Specific Root Length (SRL) total root length/root dry biomass (cm g^{-1}); Specific Root Area (SRA) total surface area/root dry biomass (cm^2 g^{-1}); Root Tissue Density (RTD) root dry biomass/root volume (g cm^{-3}); Root Dry Matter Content (RDMC) dry root biomass/fresh root biomass (mg g^{-1}). Plant nutrient uptake was defined as shoot nutrient content (i.e., nutrient concentration x shoot biomass) divided by root surface area (μg cm^{-2}) (Vetterlein et al. 2022). For plant tissue analysis, 150 mg of milled plant dry biomass was digested in 65% HNO_3 and 30% H_2O_2 (4:1 ratio) in a microwave digestion system (MARS 6, CEM Corporation, Matthews, USA). The concentrations of P, K, Zn, Mn and Mg were determined by inductively coupled plasma optical emission spectrometry (ICP-OES) (Optima 8300, Perkin Elmer, Waltham/MA, USA).

2.5. Quantitative root exudate analysis by spectrophotometry

All exudate samples were analysed with a plate reader (TECAN Infinite® 200 PRO nano) and the respective photometric assays are described below. Before analysis, samples were pre-concentrated by freeze drying a 40 mL sample aliquot (− 45 °C; 0.070 mbar, Alpha 1–4 LSCplus, Christ, Osterode am Harz, Germany) and resuspended in 2.4 mL of MQW before analysis (concentration factor: 16.7). Dissolved organic carbon (DOC) was determined photometrically according to Oburger et al. (2022b) without any sample pre-treatment. Briefly, a calibration curve was prepared using potassium phthalate (KHP, Elementar 35.00–0151) standard (0.5–40 mg C L^{-1}) dissolved in MQW water. Calibration blanks, calibration standards as well as thawed exudation samples and sample blanks (i.e., exudate sampling solution only) (250 μL) were pipetted into 96 microwell plate (Greiner UV-STAR® flat-bottom) suitable for absorbance analysis in the UV/VIS spectrum, and absorbance was measured at 260 nm. Carbon exudation rates were calculated based on RSA per hour as well as based on total root biomass allowing the determination of total DOC input per plant per hour at different developmental stages. Experimental details about the photometric assays used to characterize exudate samples can be found in the Supporting Information (SI).

Soluble carbohydrates (mono- to oligo saccharides) were determined using the anthrone method from Hansen and Møller (1975). Results were expressed as nmol of glucose equivalents.

Total phenolic concentration was determined by the Folin-Ciocalteau method (Singleton and Rossi, 1965) as described by Ainsworth and Gillespie (2007). Results were expressed as nmol of chlorogenic acid equivalents.

Total free amino acid concentration was determined fluorometrically with the o-phthalaldehyde (OPA) and β-mercaptoethanol method (Jones et al. 2002). The OPA reagent is known to interact with ammonium as well, however, NH_4^+ concentrations (determined according to Hood-Nowotny et al. (2010)) were below the limit of quantification and therefore not considered. In addition, root exudate samples did not show autofluorescence, thus autofluorescence was not accounted for amino acids quantification. To compensate for quenching, 10 μL alanine standard (100 μmol L^{-1}) was spiked to a second aliquot of exudate samples and then compared with spiked method blanks (MQW plus OPA reagent); the recovery factor was included in the final equation to calculate amino acid concentration. Results were expressed as nmol alanine equivalents.

Protein content of the exudate samples was determined by the dye-binding method of Bradford (1976), using Coomassie Protein Assay Kit (Thermo Scientific, Waltham, MA, USA) and Bovine Serum Albumin (BSA) as calibration standard (1–25 μg mL^{-1}). After determination of the target analyte concentration by the respective assay and accounting for sample pre-concentration and original sample volume, exudation rates were calculated based on cm^2 RSA per hour (based on the sampling duration). The relative contribution of each exudate compound class to the total DOC exuded was estimated by multiplying the measured compound concentration (mol L^{-1}) per sampling volume (L) and number of C atoms of the standard used for the calibration of the respective photometric assay (i.e., 6 C atoms for sugars (glucose), 16 C atoms for phenolic compounds (chlorogenic acid)). For the amino acids assay, 5 C atoms were used (the median of the C atom presents in the 20 amino acids naturally occurring in proteins).

2.6. LC-HRMS sample preparation and non-targeted analysis

Exudate sample aliquots (40 mL) stored at − 80 °C were freeze-dried (− 45 °C; 0.070 mbar, Alpha 1–4 LSCplus, Christ, Osterode am Harz, Germany), reconstituted in 1.2 mL MQW and filtered with 0.2 μm filters (4 mm; cellulose acetate, Nalgene™, USA) (Lohse et al. 2023). Two different chromatographic separation methods, namely reversed phase liquid chromatography (RPLC) and hydrophilic interaction liquid chromatography (HILIC), were used for the non-targeted metabolomic analyses. Reconstituted samples were diluted 1:2 with MQW for RPLC, while in HILIC, the reconstituted samples were diluted 1:4 with ACN before the measurement, as described in Lohse et al. (2023). Quality control samples (QC) were prepared by pooling 40 μL of each sample together and injected every five samples to monitor the stability LC-QTOMS system. Replicates from the same treatment (i.e., L-WT, L-*rth3*, S-WT, S-*rth3* and sample blank) and same BBCH were pooled together and injected as unique sample (n = 20) in a randomized sequence. Chromatographic separation was performed using an Infinity II UHPLC system (Agilent Technologies, Santa Clara, USA). Analytical columns from Waters Corporation (Milford, USA) were utilized in this study, namely an Atlantis T3 C18 (2.1 ×150 mm, 3 μm particle size) and a Xbridge BEH amide® (2.1 ×150 mm, 3.5 μm particle size). MS detection was performed on the 6560 IM-QTOFMS from Agilent Technologies equipped with a Dual Jetstream ESI interface. Agilent Mass Hunter Acquisition software (10.1) was used for instrument control. Detailed information about chromatographic separation and QTOFMS settings are shown in Table S3. For QTOFMS detection, mass range between 90 and 1700 *m/z* were recorded in positive (+) and negative (-) polarity for both HILIC and RPLC. The 2 GHz extended dynamic range mode with a spectral acquisition rate of 2 Hz was used for all measurements. The instrument tuning and mass calibration procedures were carried out in accordance with the guidelines provided by the manufacturer. The fragmentation data were acquired in Data Dependent Analysis mode (DDA), with a narrow isolation window (1.3 *m/z*) for the precursor isolation. The collision energies were calculated for each precursor ion according to the following equation: Collision energy = (slope x *m/z* of precursor mass)/100 + Offset.

2.7. LC-MS raw data processing

MassHunter Profinder B.10.00 software (Agilent Technologies, Sta Clara, CA) was used for peak integration and chromatographic deconvolution with a Batch Recursive Feature Extraction (BRE, small molecules/peptides) workflow (for details see SI of Lohse et al. (2023)). Briefly, the extracted features were aligned across the samples according to *m/z* and retention time; mass accuracy and retention time tolerance were set at ± 5 ppm and ± 0.30 min, respectively. Data was checked manually in terms of correct integration and peak assignment. Missing values were replaced by 1, and then raw intensities were scaled according to RSA/sampling volume ratio. Only features showing a fold change > 10 compared to sample blanks of the respective BBCH were further processed. Exact mass and retention time, together with MS/MS fragmentation spectra were used to identify compounds by matching with an in-house standard mix MS/MS library, online spectral libraries and MS^2 databases (e.g., Metlin (https://metlin.scripps.edu/), MoNA (https://mona.fiehnlab.ucdavis.edu/)) using the NIST MS search program v.2.4 (National Institute Standard and Technology (NIST), Scientific Instrument services, Inc., NJ, USA) using the NIST20 mass spectral database and other available libraries imported in the NIST MS search program software. For each of the identified metabolites, we assigned a level of confidence according to Schymanski et al. (2014). Definitions of confidence level can be found in the SI to this paper. The identified compounds, matched fragments, the identification level, and analytical method used are reported in the support material of this manuscript (SI Excel Table).

2.8. Statistical analysis

The experimental setup, including the sampling procedure, followed a completely randomized design. Data are expressed as mean ± standard error (SEM). Exudation rates were normalized on RSA. Univariate statistical analysis, principal component scores for root traits and graphs were constructed using Graphpad Prism 9.4.1 for Windows (GraphPad Software, San Diego, CA, USA). Raw data were log transformed prior to analysis. A two factorial ANOVA, followed by the Tukey's HSD multiple comparison test was used to test the difference between means of different treatments for plant biomass, root morphological parameters, and plant total C exudation. A 3-way ANOVA was used to assess the variation in exudation rates between substrates, genotypes, and developmental stages. Root traits data were log transformed and standardized (i.e., mean = 0 and standard deviation = 1) prior analyses. Correlations between root traits were assessed using Pearson's correlation. Differences between tested treatments were considered significant at $p \leq 0.05$. Multivariate statistical analyses as Principal Component Analysis (PCA), and Orthogonal Projection to latent structures Discriminant Analysis (OPLS-DA) of LC-QTOFMS data were performed using SIMCA 17.0.2 software (Umetrics, Umeå, Sweden). Before modelling, metabolomics data were scaled according to RSA/sampling volume ratio, log transformed, and then further scaled to unit variance (UV-scaling). The quality of the models was described by R^2 (goodness of fit) and Q^2 (predictability) statistics. OPLS-DA models were automatically fitted to determine the number of significant components. Validation plots of the OPLS-DA models were confirmed by 100 permutation tests. The Variable Importance of Projection (VIP) (Eriksson et al. 2013; Galindo-Prieto et al. 2014) was used to determine the discriminatory power of each variable explaining the differences between classes in the OPLS-DA models. The plant grown in the field plot 08 (L-*rth3*) at BBCH 83 was already dead at the day of harvest. The sample from field plot 17 (S-WT) at BBCH 14 had only one plant on the harvest day and was thus removed from further data evaluation as the RSA/sampling volume ratio significantly differed compared to the other treatments.

3. Results

3.1. Biomass and root traits

We used custom-made soil columns to cultivate and harvest maize plants in the field, preserving their intact root systems and allowing us to collect root exudates at four different growth stages. Both root and shoot biomass showed differences depending on substrate and genotype (Table 1), being generally lower for the *rth3* root hairless mutant than WT and for S-grown plants when compared to L. Nonetheless, these differences were not always consistently statistically significant (Table 1). Overall, substrate had the greatest effect on maize plant biomass production, particularly at later growth stages (BBCH 19, 59, 83) irrespective of plant tissue type, while genotype only occasionally drove differences in either root or shoot biomass at individual growth stages (shoot: BBCH 19, 59, root: BBCH 14, 83) (Table 1). Despite the absence of root hairs in *rth3* resulted in a reduced absorption surface, we did not observe any evidence of a higher C investment in root biomass in *rth3* compared to WT, but rather the opposite with WT showing a higher root:shoot ratio compared to *rth3* at BBCH 14 and BBCH 83 (Table 1). At BBCH 14, when the plants were still relatively small, the differences in nutrient tissue concentrations between genotypes and substrates were negligible. Starting from BBCH 19, plants grown in L showed higher tissue concentration of P and Zn, while no substrate difference was observed for K, Mn and Mg (Table S4). Concurrently, genotype had a significant effect only on P and K concentration. Interestingly, P tissue concentrations were higher in *rth3* plants, while WT plants showed higher level of K.

In contrast to root biomass, root morphological traits were mostly

Table 1
Biomass of maize (Zea mays L., WT and rth3) plants grown on two substrates (loam and sand), across different plant developmental stages (BBCH 14, BBCH 19, BBCH 59, BBCH 83), under field conditions. Differences between treatments (i.e., substrate and genotype) within each BBCH were evaluated by 2-way ANOVA including Tukey's post-hoc test. Means with different letters are statistically different ($p < 0.05$). * ** represents $p < 0.001$; * *$p < 0.01$; * $p < 0.05$; ns = not significant, values represent means ± SEM (n = 4; BBCH 14 S-WT and BBCH 83 L-rth3 = 3).

	Treat.	Root dry Biomass (g)	Shoot dry biomass (g)	Root/shoot ratio
BBCH 14	L-WT	0.35 ± 0.03 a	0.32 ± 0.03 a	1.10 ± 0.04 ab
	L-*rth3*	0.17 ± 0.02 a	0.19 ± 0.01 a	0.91 ± 0.06 ab
	S-WT	0.27 ± 0.08 a	0.19 ± 0.03 a	1.40 ± 0.26 a
	S-*rth3*	0.20 ± 0.04 a	0.19 ± 0.04 a	1.10 ± 0.11 b
p-value (ANOVA)	Substrate	ns	ns	*
	Genotype	*	ns	*
	Interaction	ns	ns	ns
BBCH 19	L-WT	3.3 ± 0.4 a	3.6 ± 0.4 a	0.96 ± 0.15 a
	L-*rth3*	1.5 ± 0.3 ab	1.5 ± 0.2 ab	0.96 ± 0.15 a
	S-WT	1.3 ± 0.3 ab	1.4 ± 0.3 b	0.94 ± 0.06 a
	S-*rth3*	1.2 ± 0.5 b	1.1 ± 0.3 b	1.0 ± 0.1 a
p-value (ANOVA)	Substrate	*	* *	ns
	Genotype	ns	*	ns
	Interaction	ns	ns	ns
BBCH 59	L-WT	17.0 ± 1.5 a	33.0 ± 5.0 a	0.52 ± 0.04 b
	L-*rth3*	8.8 ± 1.4 b	17.0 ± 2.6 b	0.53 ± 0.04 b
	S-WT	8.5 ± 0.9 b	13.0 ± 1.4 bc	0.66 ± 0.03 ab
	S-*rth3*	6.3 ± 1.1 b	8.1 ± 1.4c	0.78 ± 0.04 a
p-value (ANOVA)	Substrate	* *	* **	* **
	Genotype	* *	* *	ns
	Interaction	ns	ns	ns
BBCH 83	L-WT	16.0 ± 1.9 a	34.0 ± 4.0 a	0.49 ± 0.04 a
	L-*rth3*	12.0 ± 0.2 ab	32.0 ± 4.3 a	0.38 ± 0.05 a
	S-WT	9.0 ± 1.0 bc	22.0 ± 2.5 ab	0.41 ± 0.01 a
	S-*rth3*	6.2 ± 0.3 c	17.0 ± 1.7 b	0.36 ± 0.02 a
p-value (ANOVA)	Substrate	* **	* *	ns
	Genotype	* *	ns	*
	Interaction	ns	ns	ns

influenced by genotype rather than substrate. We observed the same trend for root length (RL), root surface area (RSA) and root volume (RV), where the WT genotype was always significantly higher than its root hairless mutant *rth3* (Table S5). We did not detect differences in root morphological parameters between substrates, except for the latest growth stage (BBCH 83), where L substrate showed higher RL, RSA and RV (Table S5).

Multivariate data analysis revealed that root functional traits differed strongly between plant developmental stages and substrates (Fig. 2a) with the first 2 components explaining altogether more than 82% of the total variation. Traits such as root tissue density (RTD) and root dry matter content (RDMC) were higher at later growth stages and were positively correlated to K and P uptake. Specific root length (SRL) and specific root area (SRA) were higher in S especially at BBCH 14 and 19. Carbon exudation rates (Exu rate) were higher in *rth3* particularly at early growth stages and positively correlated to root diameter (RD) and root:shoot ratio (R:S), while it was inversely correlated to RTD and K uptake (Fig. 2b).

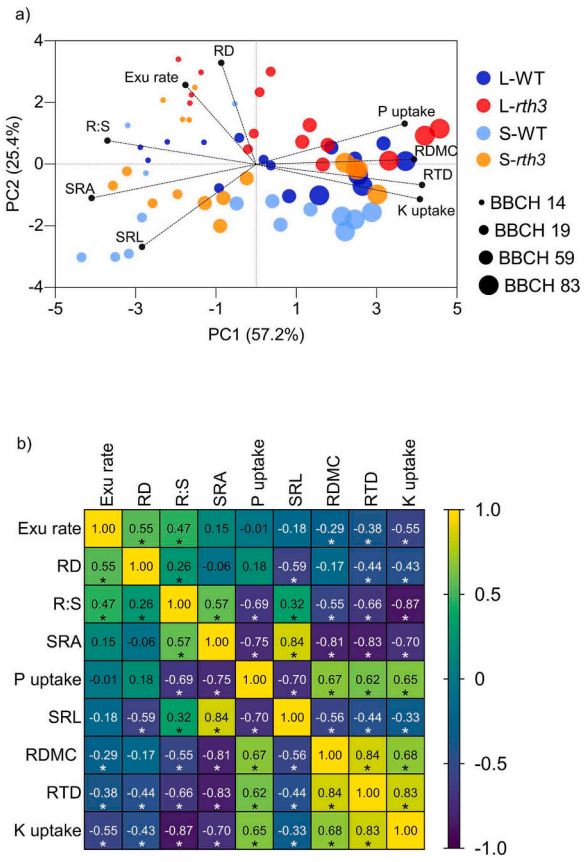

Fig. 2. Changes in root traits of maize (Zea mays L., WT and *rth3*) grown on two substrates (Loam and Sand), across different plant developmental stages (BBCH 14, BBCH 19, BBCH 59, BBCH 83), under field conditions. (a) PCA biplot. Dashed lines on PCA indicate projections for each root trait. Circle size indicates different BBCH, L: loam, S: sand, colours represent different treatments (L-WT: blue, L-*rth3*: red, S-WT: cyan, S-*rth3* orange). Root trait annotations are as follows: RD – root diameter; SRA – specific root area; P uptake – phosphorus plant uptake per unit surface area; K uptake – potassium plant uptake per unit surface area; RTD – root tissue density; SRL – specific root length; R:S – root:shoot ratio; Exu rate – hourly exuded carbon per cm^2 root surface area; RDMC – root dry matter content. (b) Pearson correlation coefficients of root traits. Root traits were sorted in descending order based on the correlation with root exudation. Asterisks indicates correlations with p-value < 0.05. Root trait values used in the PCA can be found in Table S8.

3.2. Carbon exudation

C exudation rate of root hairless *rth3* and the corresponding WT showed marked differences in exudation patterns for each experimental factor (i.e., substrate, genotype and developmental stage, Fig. 3a). C exudation rates (μmol C cm^{-2} RSA h^{-1}) decreased over time with plant development (except BBCH 19, L-*rth3*), ranging from 0.57 μmol C cm^{-2} h^{-1} (L-WT, BBCH 19) to 0.12 μmol C cm^{-2} h^{-1} (S-WT, BBCH 83). Plant growth stage accounted for the highest percentage of explained variation (43.7%, Fig. 3a). Interestingly, *rth3* hairless mutant always showed a higher exudation rate than its WT sibling within the same substrate and growth stage ($p = 0.0074$, Fig. 3a). Furthermore, C exudation rates were always higher in L compared to exudation rates observed in S, irrespective of genotype ($p = 0.0134$, Fig. 3a). Calculating the C release per plant per hour at each growth stage (mmol C per plant h^{-1}, Fig. 3b), revealed that substrate was the main driver of differences in C input in BBCH 19, 59 and 83, while C release at the earliest growth stage (BBCH 14) was mostly affected by genotype. In line with observed exudation rates, we found greater plant C input in L than in S. However, while C exudation rates were always greater in *rth3* than in WT, C input into the

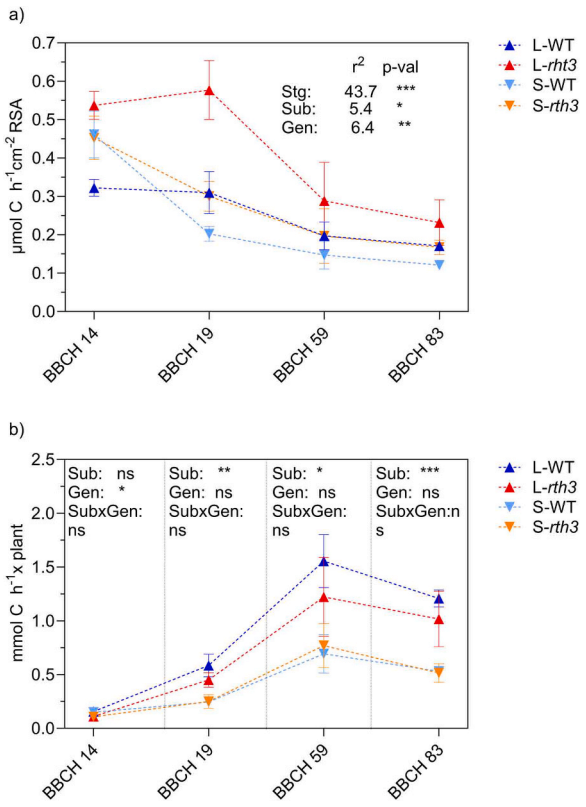

Fig. 3. Root C exudation of maize (Zea mays L., WT and rth3) grown on two substrates (Loam and Sand), across different plant developmental stages (BBCH 14, BBCH 19, BBCH 59, BBCH 83), under field conditions. L: loam, S: sand, colours represent different treatments (L-WT: blue, L-rth3: red, S-WT: cyan, S-rth3 orange), symbols indicate different substrates (▲: loam,▼: sand). (a) C exudation rate (µmol C cm^{-2} RSA h^{-1}). Differences between experimental factors (i.e., growth stage (stg), substrate, and genotype) were evaluated by 3-way ANOVA Analysis of Variance. (b) C input into soil per plant (mmol C $plant^{-1}$ h^{-1}). Differences between experimental factors (i.e., substrate, and genotype) were evaluated within each BBCH separately with 2-way ANOVA Analysis of Variance. * ** $p < 0.001$, * *$p < 0.01$ * , $p < 0.05$, ns = not significant. Values represent means ± SEM. (n = 4; BBCH 14 S-WT and BBCH 83 L-rth3 = 3).

soil per plant was higher in L-WT due to greater root biomass production than L-*rth3*. No differences for plant C input could be observed between S-WT and S-*rth3*.

3.3. Root exudation of different compound classes

To characterize quantitative differences in soluble carbohydrates, amino acids, proteins, and phenolic compounds we applied a range of well-established photometric methods. Results showed the same trend as we already observed in total C exudation, irrespective of compound class investigated, with exudation rates (per cm^2 RSA) declining with progressing plant development and higher exudation rates in *rth3* than in WT (Fig. 4). Like C exudation, plant developmental stage was the main driver explaining the highest portion of variation (26–53%) in each of the compound classes analysed. The difference between substrates was significant only for phenolics, being evident mostly at BBCH 83 (Fig. 4b), where exudation rate of L grown plants was higher than the S grown ones. Genotype effect was statistically significant for all the three compound classes explaining between 5% and 10% of the observed variation, with the *rth3* mutant having generally higher exudation rates compared to WT, particularly during the vegetative growth (BBCH 14 and 19). Protein exudation (Fig. 4d) reflected the same growth stage dependent decreasing trend observed in the other compound classes, with the highest exudation rate measured in S-WT BBCH 14 (88.5 µg protein cm^{-2} RSA h^{-1}). Protein concentration was below the limit of quantification in L-*rth3*, S-WT, and S-*rth3* at BBCH 83. Estimating the relative C contribution of each compound class to the total C exudation revealed that the relative contribution of phenolic compounds and amino acids (mean across all treatments and developmental stages) remained rather similar across treatments and plant developmental stages (Fig. 5a, b). The contribution of carbohydrates first decreased from BBCH 14 to 19 and then increased over time contributing for more than 50% of C exudation in L-WT at BBCH 83. Overall, the sum of C derived from the three compound classes accounted from a minimum of 24% (L-WT, BBCH 19) up to 62% (L-WT, BBCH 83) of total organic C exuded, leaving a significant amount of C uncharacterized by our spectrophotometric approach (Fig. 5a, b).

3.4. Non-targeted metabolomics analyses of root exudates

Non-targeted analyses of the metabolome were performed to investigate the three experimental factors, i.e., plant developmental stage, substrate, and genotype. The number of molecular features passing the quality control filters for the HILIC method were 157 and 144 for negative and positive ionization respectively, whereas RPLC method resulted in a higher number of molecular features, consisting in 397 for the negative ionization and 313 for the positive. PCA score plots (Fig. S2) of metabolite data revealed that clustering of root exudates was mostly based on plant developmental stage. Substrate-driven clustering could also be observed to a minor extent, depending on the analytical approach and growth stage (e.g., HILIC (-) and RPLC (-)/(+) at BBCH 83 (Fig. S2). The two first principal components (R2X[1] and R2X [2]) of the PCA analysis explained 55% (RPLC(-)), 62% (RPLC (+)), 66% (HILIC (+)) and 56% (HILIC (-)) of the variation in the datasets, respectively (Fig. S2). To further investigate the differences in root exudation patterns, we performed supervised OPLS-DA analyses assessing the different growth stages (BBCH) (i.e., the experimental factor explaining the highest variation in the exudation dataset) as model classes. Detailed information on the OPLS-DA models parameter (e.g., R^2 and Q^2) can be found in the SI, Table S7. Unlike PCA, OPLS-DA projections are guided by known class information, leading to a maximum separation model instead of the maximum variation model (i.e., PCA). Irrespective of analytical approach, we found a clear separation between BBCH 83 and 59, while BBCH 19 and 14 were still partially overlapping, highlighting the similarity between these two datasets (Fig. 6). The predictive component of the OPLS-DA models (t[1] component, x-axis) explaining the variation between the growth stages (BBCH) was similar for all the 4 methodological approaches used for root exudates analysis, ranging from 32% of HILIC (-) to 49% of RPLC (+) (Fig. 6a, b, c, d R2X[1]; Table S7). The modelled variation in the orthogonal component (i.e., within BBCHs) was lower compared to the predictive one (i.e., between BBCHs), regardless the methodological approach used for the non-targeted analysis (11% RPLC (+)/(-), 20% HILIC (-) and 28% HILIC (+) (Fig. 6a, b, c, d] R2Xo[1], Table S7). To test the suitability of the OPLS-DA to model the variation determined by genotype and substrate as experimental factors, we tested both as OPLS-DA model classes. Results showed that OPLS-DA based on genotype led to significant components only in RPLC, modelling only 3% of the total variation (Table S7), while substrate factor accounted for the 11% of variation in HILIC (+) and both RPLC (-) and RPLC (+), showing no significant component in HILIC (-) (Table S7). These results were thus consistent to the 3-way ANOVA results (Fig. 3a), displaying plant growth stage as the main factor driving root exudation patterns in field grown maize plants, with genotype and substrate accounting for roughly 10% of the variance, altogether. Due to the high number of detected molecular features (1011, sum of the features detected by the four analytical methods), we prioritized the top 50 molecular features (from each analytical method) with the highest VIP score, representing a high discriminatory power for BBCHs. Fig. 7 summarizes the relative abundance of the annotated

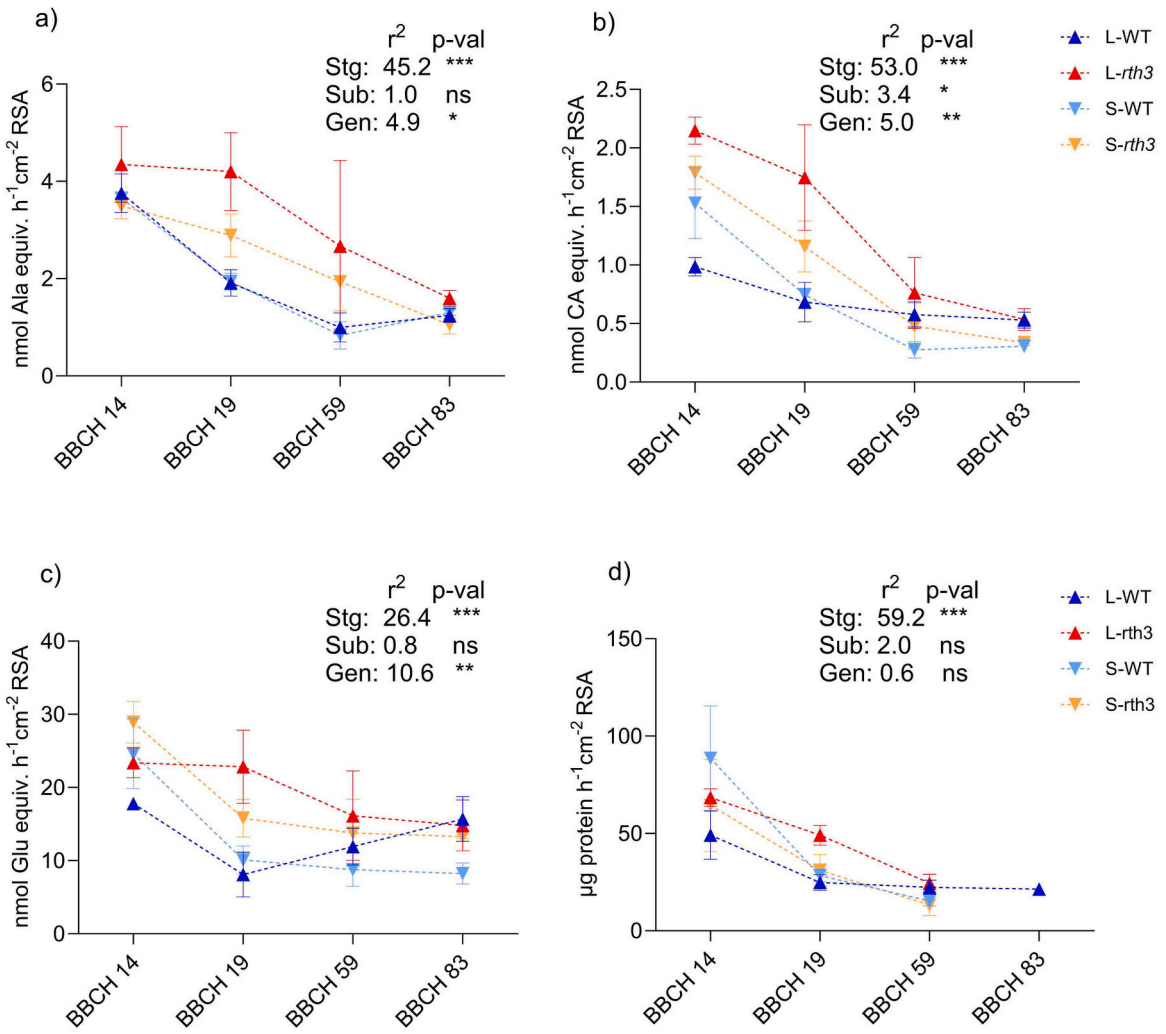

Fig. 4. Exudation rates of different compound groups of maize (Zea mays L., WT and rth3) grown on two substrates (Loam and Sand) across different plant developmental stages (BBCH 14, BBCH 19, BBCH 59, BBCH 83) under field conditions. L: loam, S: sand, colours represent different treatments (L-WT: blue, L-rth3: red, S-WT: cyan, S-rth3 orange), symbols indicate different substrates (▲: loam,▼: sand). (a) Amino acids (nmol alanine equiv. cm-2 RSA h-1). (b) Phenolic compounds (nmol chlorogenic acid equiv. cm^{-2} RSA h^{-1}). (c) Soluble carbohydrates (nmol glucose equiv. cm^{-2} RSA h^{-1}). (d) Proteins (µg protein cm^{-2} RSA h^{-1}) Differences between experimental factors (i.e., growth stage (stg), substrate, and genotype) were evaluated by 3-way ANOVA * ** $p < 0.001$, * *$p < 0.01$ * , $p < 0.05$ ns = not significant. Values represent means ± SEM (n = 4; BBCH 14 S-WT and BBCH 83 L-rth3 = 3).

compounds for each growth stage, substrate, and genotype irrespective of the analytical approach applied. A detailed list of the top 50 molecular features (i.e., neutral mass and retention time) resulting from the respective analytical method can be found in the SI, Excel table. In line with what we observed for C exudation, the relative abundance of most of the annotated compounds decreased with increasing plant age. Interestingly, some metabolites also showed higher abundance at BBCH 59 and 83, including several sugars and sugar derivatives (e.g., monosaccharides and disaccharides), benzoxazinoids such as 2,4-dihydroxy-1,4-benzoxazin-3-one (DIBOA) and DHBOA-Glc, and the N-trimethyl-4-aminobutyric acid (N-trimethyl GABA). Few metabolites were found to be unique for a specific growth stage. Esculetin, for example, was only found at BBCH 19 and was only detected in L. Also, chlorogenic acid was only detected at BBCH 19, while the 3,4-dihydroxy-3-oxo-2 H (1,4)-benzoxazin-ʏ lactic acid was only found at BBCH 14. In line with C exudation rates (Fig. 3a), general trend of higher relative abundance of annotated metabolites was found in *rth3* compared to WT maize genotype as well as in L when compared to the S substrate (Fig. 7).

4. Discussion

4.1. Plant developmental stage was the strongest driver for observed differences in root exudation patterns

Our findings revealed that plant development was the main contributor among the investigated experimental factors for shaping root exudation patterns. It accounted for the highest variation in the exudation rates of C, targeted compound groups (i.e., phenolics, soluble carbohydrates, amino acids, and proteins), and in detected metabolite profiles (Fig. 3a, Fig. 4, Fig. 6, Fig. 7). Generally, exudation rates for C and specific compound classes (Fig. 3a, Fig. 4, Fig. 5b) decreased with plant development, except for sugars and amino acids in L-WT (Fig. 4a, c). Our results are consistent with the literature and in line with our expectations of exudation rates being higher for juvenile plants. Ganther et al. (2022) also reported higher levels of assimilated ^{13}C and enhanced expression of growth-related genes at BBCH 14 than at BBCH 59 in the same field experiment. This indicates a more active C metabolism in the exponential growth phase which was also reflected in higher exudation rates. Several other studies also reported a strong effect of plant development on the extent and composition of root exudation. Most of these

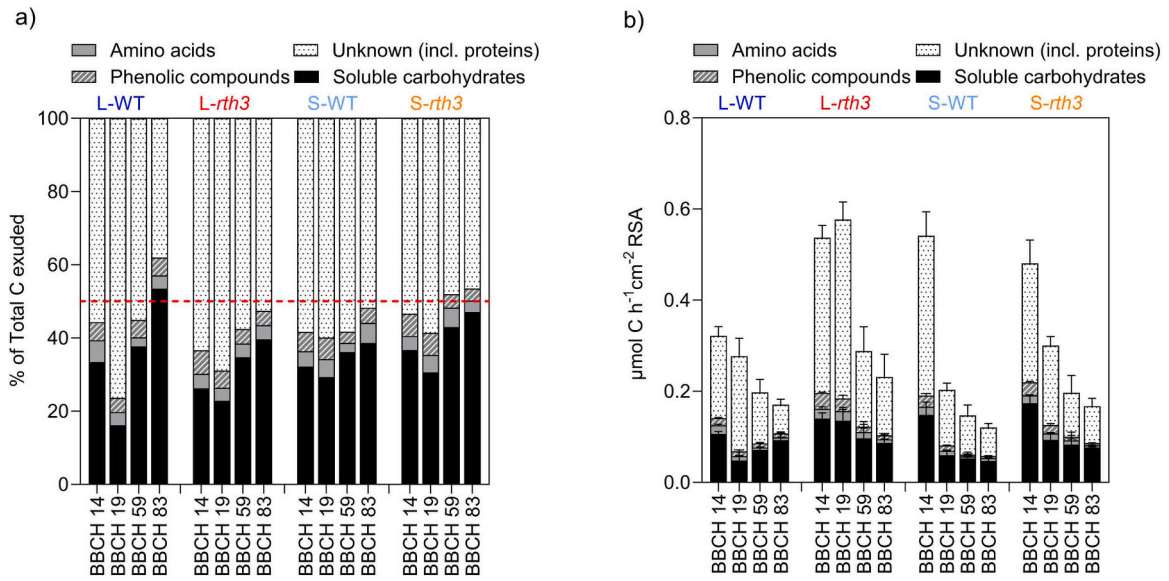

Fig. 5. Estimation of the relative contribution of different exudate compound groups to the total C exudation of two maize genotypes (Zea mays L., WT and rth3) grown on two substrates (Loam and Sand) across different plant developmental stages (BBCH 14, BBCH 19, BBCH 59, BBCH 83) under field conditions, L: loam, S: sand. (a) Normalized compound group exudation. The concentration of each compound group was normalized to the total µmol C exudation, ranging between 0 and 100, with 100 representing the total C exuded within the respective treatment and growth stage. Values represent means of each treatment (i.e., L-WT, L-rth3, S-WT, S-rth3). The dotted line was added as visual reference and marks the 50%. (b) Compound group derived C exudation rate. The sum of the estimated compound group exudation rate is equal to the total C exudation rate of the respective treatment and BBCH. Values represent means ± SEM (n = 4; BBCH 14 S-WT and BBCH 83 L-rth3 = 3).

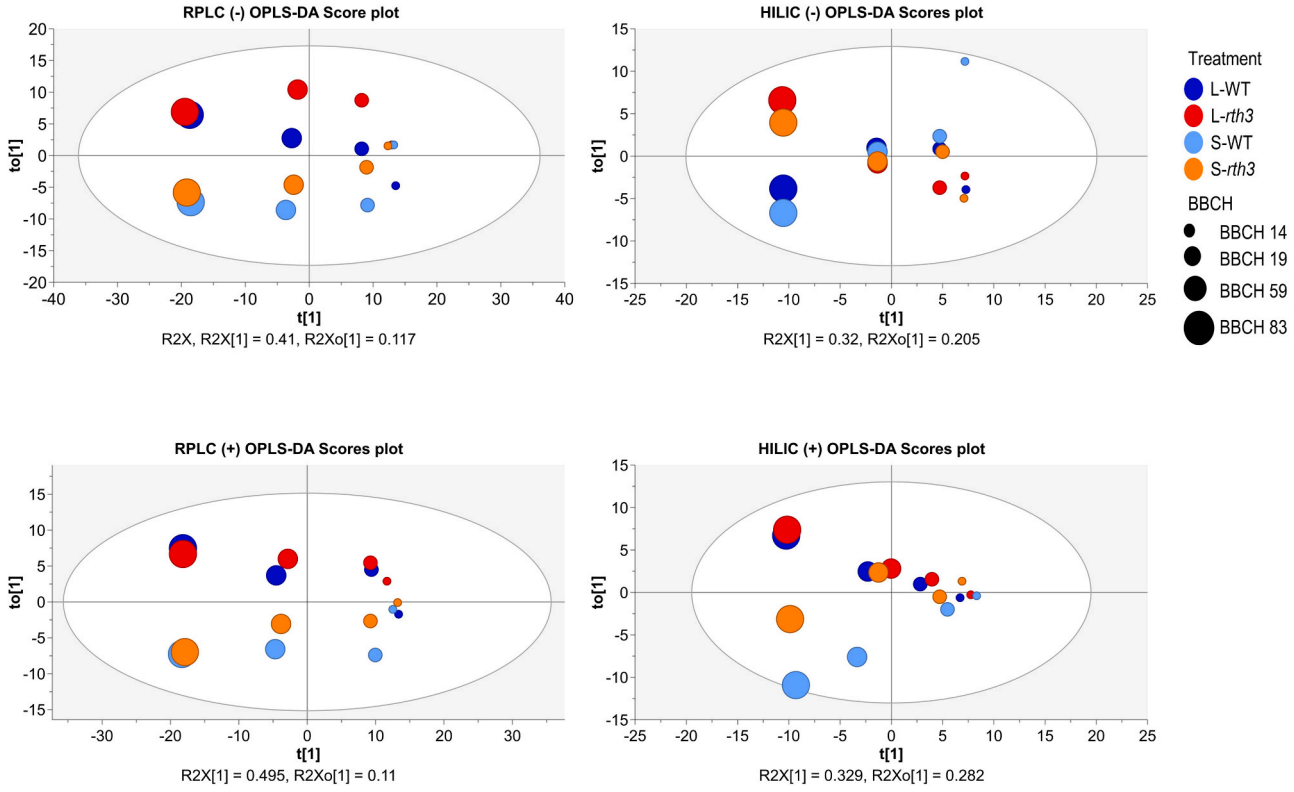

Fig. 6. OPLS-DA scores plot of root exudate metabolomic data of two maize genotypes (Zea mays L., WT and rth3) grown on two substrates (loam and sand) across different plant developmental stages (BBCH 14, BBCH 19, BBCH 59, BBCH 83) under field conditions. Circle size indicates different BBCH, L: loam, S: sand, colours represent different treatments (L-WT: blue, L-rth3: red, S-WT: cyan, S-rth3 orange). OPLS-DA score plots show the variation explained by the first component of the model both the predictive t[1] (R2X[1] i.e. between groups) and orthogonal to[1] (R2Xo[1] i.e., within groups). Samples from the same treatment (i.e., L-WT, L-rth3, S-WT, S-rth3), and BBCH were pooled together before metabolomic analysis. Ellipse indicates the confidence region (95%), (n = 16; BBCH 14 = 4, BBCH 19 = 4, BBCH 59 = 4, BBCH 83 = 4). Details of the OPLS-DA models performance can be found in Table S7.

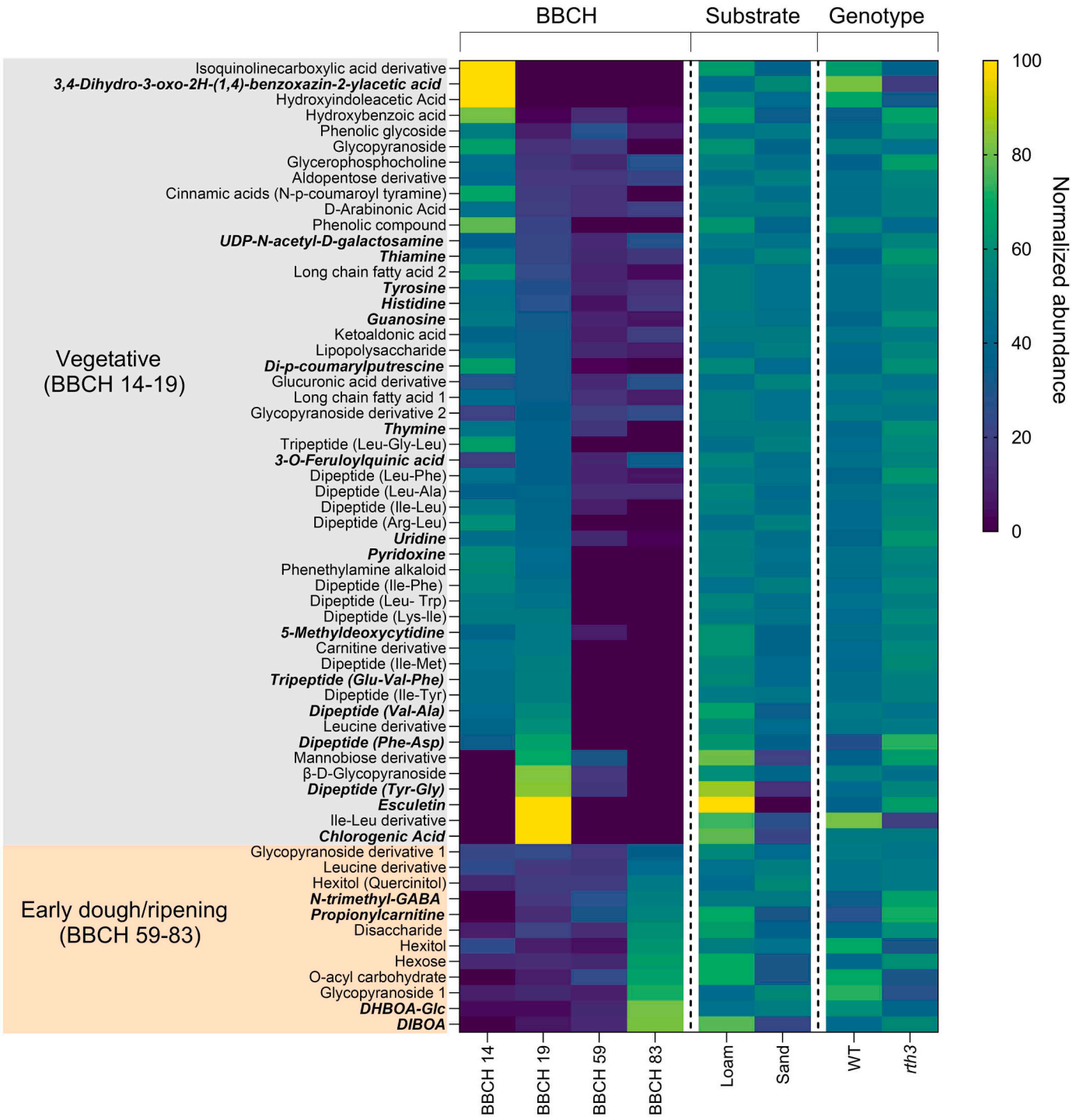

Fig. 7. Changes in the relative abundances of root exuded annotated metabolites of two maize genotypes (Zea mays L., WT and rth3) grown on two substrates (loam and sand) across different plant developmental stages (BBCH 14, BBCH 19, BBCH 59, BBCH 83) under field conditions. All abundances derived from LC-QTOFMS analyses were normalized to a range between 1 and 100, with 100 representing the sum for each metabolite released within the respective experimental factor (i.e., BBCH, substrate, and genotype) (n = 16). Metabolites having the highest relative abundance at BBCH 14 or 19 were grouped together in the vegetative group. Metabolites having the highest relative abundance at BBCH 83 were grouped together in Early dough/ripening group. Metabolites were then sorted ascendingly within the respective group based on the BBCH 19 and BBCH 83 relative abundances. BBCH-derived metabolite order was kept the same for presented normalized abundances of the two substrates (across all BBCHs and genotypes) and the two genotype (across all BBCHs and substrates). Depicted compounds were identified with a confidence level range from 1 to 3. Metabolites in italic bold were annotated with a confidence level of 1 or 2 (see SI, Definition of confidence level). For compounds with a level of confidence of 3 the respective compound class is given. Information about the identification confidence, mass, retention time, matched ion fragments and analytical method used for each compound can be found in the SI, Excel table.

studies (except Aulakh et al. (2001) and Lucas García et al. (2001)) were conducted under hydroponic or semi-hydroponic conditions (Chaparro et al. 2013; Gransee and Wittenmayer, 2000; Zhalnina et al. 2018). Evidence from those studies (irrespective of plant growth medium) also suggests that an actively growing root system secretes more exudates than a physiologically less active one (e.g., during early dough or ripening). Plants have a higher nutrient and water demand in their vegetative growth phase than during flowering/fruiting and seem to adjust exudation patterns to favour nutrient mobilization and microbial recruitment. Considering that passive diffusion is (thought to be) a strong driver of exudation (Canarini et al. 2019), observed changes in exudation with plant development might also simply be - at least partly - a "by-product" of C partitioning dynamics during the plant's life cycle. However, to date the exact mechanisms of root exudation dynamics remain to be revealed. When converting exudation results (presented on a per plant basis) from soil-grown rice (*Oryza sativa* L.) cultivars to C exudation rates normalized by root biomass, Aulakh et al. (2001) also found a decrease in exudation with increasing plant development. The study of Aulakh et al. (2001) is one of very few reports investigating root exudation of soil grown crops throughout the whole plant life cycle and to the best of our knowledge, no data on field-based studies for maize root exudation are available yet.

In addition to changes in C exudation rates with time, we also found plant developmental-driven changes for individual metabolites such as benzoxazinoids (i.e., DIBOA, DHBOA-Glc), B vitamins (i.e., thiamine, pyridoxine), phenolics (e.g., organic acids), amino acids, carbohydrates and their derivatives (Figs. 4, 7), with many of these metabolites being implicated in actively shaping the associated rhizobiome (Hu et al. 2018; Neal et al. 2012; Stringlis et al. 2018; Wang et al. 2022). Also, defence-related metabolites (i.e., DIBOA, DHBOA-Glc) were up-regulated in the vegetative-to-floral transition and the subsequent on-set of flowering (Fig. 7). Gransee and Wittenmayer (2000) characterized root exudates of maize and pea (*Pisum sativum* L.) plants grown in quartz sand by coupling ^{14}C labelling with ion exchange chromatography and reported a decrease of sugars, amino acids, and total C derived radioactivity per g root dry biomass in the exudates of maize plants at 8 leaves stage compared to 4 leaves stage. Higher cumulative exudation levels of sugars and sugar alcohols have also been reported in *Arabidopsis* root exudates for early time points (i.e., 8–10 days old) compared to later ones (i.e., 22–30 days old), while the amino acids and phenolics (e.g., organic acids) followed the opposite trend (Chaparro et al. 2013; Zhao et al. 2021). However, the data presented in this study (i.e., Chaparro et al. (2013)) was not normalized for root biomass (or root surface area) which might bias obtained results as roots continue to grow with time. As emphasized by Oburger and Jones (2018), normalization strategies for exudation data are quite diverse, and the choice of how exudation data are presented might lead to different interpretations of the same experiment. For instance, in this experiment exudation rates per unit root surface area (μmol C cm^{-2} RSA h^{-1}) decreased with plant development (Fig. 3a) but the total C input per plant into the soil (μmol C h^{-1} x plant) was strongly dependent on the extent of the root system (Fig. 3b). Thus, overall older plants with a bigger root system exuded more C into the rhizosphere compared to younger plants, increasing the volume of soil affected by root exudation. When expressed on a per plant basis, observed C exudation dynamics per maize plant followed the same trend as reported for rice with C release being lowest at the seedling stage, peaking at flowering and declining at maturity (Aulakh et al. 2001).

Composition and concentration of root exudates were reported to vary based on the specific environmental conditions the plant is experiencing (Chaparro et al. 2013; Flores et al. 1999). The growing season of 2019 at the field research station in Bad Lauchstädt was characterized by high temperatures and low precipitation in summer, and plants experienced drought as the growing season advanced (Jorda et al. 2022; Vetterlein et al. 2022). Several studies in the past investigated the effect of drought on root exudates of different plant and tree species (Canarini et al. 2016; Gargallo-Garriga et al. 2018; Karlowsky et al. 2018; Tiziani et al. 2022; Vives-Peris et al. 2017), reporting contrasting results for C exudation and composition. This suggests that drought induces changes in the amount and composition of root exudates are species-specific and influenced by the severity of drought stress (Williams and de Vries, 2020). Plants acclimate to water deficit by changing their carbon usage, accumulating K^+ and soluble metabolites such as amino acids and carbohydrates for osmotic adjustment (Hummel et al. 2010), while conversely, roots were found to release solutes to lower the soil water potential (Karlowsky et al. 2018). For instance, elevated concentrations of hexoses in grass exudates may indicate more active mucilage production (Sinha Roy et al. 2002), whereas Gargallo-Garriga et al. (2018) reported an exudation shift toward drought stress-related secondary metabolites in *Quercus ilex*. The higher K uptake and tissue concentration, the increasing contribution of carbohydrates to the exuded C (Fig. 5a), as well as the higher relative abundance of carbohydrates and their derivates observed in this study in the older plants (Fig. 7), suggest them as possible adaptation mechanisms adopted by the plants to face the drought experienced in the later stages of the 2019 growing season.

Plant developmental stage as well as environmental conditions were also found to affect root morphology and might therefore also shape root exudation dynamics (Ostonen et al. 2007; Wells and Eissenstat, 2002). Among root traits, Specific Root Length (SRL) is probably the most frequently measured parameter as it characterizes the economic aspect of the root system (Leuschner et al. 2004; Ostonen et al. 2007) and has been reported to be correlated to higher exudation per unit of root mass (Meier et al. 2020). While we found a significant positive correlation of RD and R:S ratio with C exudation rate, our results did not confirm a significant relationship between root exudation rate and SRL or SRA, even though all four root parameters were higher in young plants (Table S8). Root Tissue Density (RTD) and Root Dry Matter Content (RDMC) increased with plant age and were negatively correlated to C exudation rate. High SRL and SRA correspond to a higher soil volume exploited per unit of biomass (i.e., resource mining) and are typically associated with a short root life span (Ryser, 2006). Contrarily, RTD and RDMC are conservative root traits associated with slower growth and higher investment in root structural functions rather than resource exploration (Birouste et al. 2014; Kramer-Walter et al. 2016), and were found to be related to low nutrient availability conditions (Aerts and Chapin, 1999; Ryser and Lambers, 1995). Generally, our results support the hypothesis of young and actively growing plants having higher nutrient demands, therefore showing fast root growth more oriented toward resource acquisition. Whether the shift toward a more conservative C belowground allocation observed in older plant is driven by environmental limitations or general plant development dynamics still requires further investigation.

4.2. *Exudation rates were higher in substrates with high sorption capacity and low nutrient mobility*

Plants grown in loam generally had higher total C exudation rates than in sand (Fig. 3a). This was also reflected in a slightly higher relative abundance of annotated metabolites (Fig. 7). Considering the higher sorption capacity in loam compared to sand (Vetterlein et al. 2021), our results suggest that low nutrient mobility triggers increased root exudation to improve nutrient exploitation. As the sand substrate was a mixture of loam with quartz sand, the physicochemical differences were less complex than when comparing two soils of different geological origin and can be roughly reduced to differences in nutrient reservoir size, sorption sites and texture. While nutrient mobility was lower in L, the nutrient reservoir potentially accessible by plants was higher compared to S (Bilyera et al. 2022; Vetterlein et al. 2021). Consequently, exploitative strategies (i.e., direct, and indirect nutrient mobilization by exudates, uptake transporter activity, change in root morphology etc.) can be expected to be more successful in L than S. The lower SRL and SRA of L grown plants suggest there was less plastic adaptation towards

soil exploration by the root system. This further supports the exploitative characteristic of root exudation (rate) as root trait (Bergmann et al. 2020; Sun et al. 2021). Conversely, the higher SRL and SRA observed for S grown plants, especially at early growth stages, indicates a higher share of fine roots for the S substrate. As these root traits are related to resource mining strategies, this suggests that S-grown plants might have adopted different strategies to forage for nutrients other than root exudation. Ganther et al. (2022) reported higher expression of genes related to mineral transport and acid phosphatase release for S-grown plants in the same field experiment, which can also be another adaptive mechanism. Other studies demonstrated that exudation differs when the same genotype is grown in soils of different geological origin (i.e., in substrates that differ in quality and quantity of plant available nutrients as well as in texture-driven nutrient mobility) (Miller et al. 2019; Neumann et al. 2014; Oburger et al. 2014). Our non-targeted metabolomics data revealed that substrate had small but significant (except for metabolites detectable by HILIC (-)) effect on the obtained metabolomics profiles (Table S7). Among annotated compounds, only a few metabolites (e.g., hexose, DIBOA, chlorogenic acid, peptides) showed significant differences between substrates (relative abundance $>$ 70%), and from the targeted compound classes only phenolics demonstrated a significant substrate effect (Fig. 4b). Root exuded phenolics have been reported to act as antibiotics and chemotactic molecules for rhizosphere microorganisms, playing roles in metal chelation and allelopathic interactions (de Weert et al. 2002; He et al. 2009; Kidd et al. 2001; Ray et al. 2018; Rudrappa et al. 2008; Steinkellner et al. 2007). Also, root exuded benzoxazinoids were reported to act as plant defence metabolites against pathogen attack and play significant role in shaping the root associated microbiome in several species (Cadot et al. 2021; Hu et al. 2018; Neal et al. 2012; Wang et al. 2022). A hydroxycoumarin (i.e., escluletin) was found to be unique to the substrate with the highest biomass production (i.e., loam) and during vegetative growth (BBCH 19), when nutrient demand was highest. Several reports identified root exuded coumarins as iron-mobilizing compounds (Clemens and Weber, 2016; Rosenkranz et al. 2021; Stringlis et al. 2019), and their accumulation in both root tissue and exudates under P-deficient conditions (Chutia et al. 2019; Ziegler et al. 2015). Generally, the small impact of substrate on exudation patterns in this study suggests that differences in substrate texture and size of the plant available nutrient reservoir had a minor effect on basic plant metabolism, and consequently on root exudation. Whether the substrate effect on exudation patterns can be expected to be greater when plants are grown in soils differing more strongly in mineralogy remains to be tested. Nevertheless, even small changes in metabolite composition may have large ecological effects, especially regarding rhizobiome composition and activity (e.g., Seitz et al. 2022; Yuan et al. 2018).

4.3. The lack of fully developed root hairs enhances exudation rates and induces changes in root morphology

In contrast to our expectations, our results revealed that C exudation rates were significantly higher for *rth3* irrespective of substrate and growth stage, and these results were further confirmed in laboratory experiments with the same maize genotypes (Lohse et al. (2023); Santangeli et al. in preparation). Microscope pictures of the WT plants (Fig. S4) demonstrate that root hairs were still present after root washing. Consequently, we can rule out that observed genotypic differences in root exudation are caused by severe damage due to our sampling procedure. Interestingly, the higher exudation rate of *rth3* plants compensated for the genotypic differences observed in root growth, leading to comparable exudation-driven total C input per plant within the same substrate (Fig. 3b). In a study conducted within the same field experiment, Ganther et al. (2022) did not find any difference in the amount of freshly assimilated ^{13}C between the two genotypes, both in the shoot and root tissues. This suggests that the higher exudation rate observed in the hairless mutant was not a result of a higher amount of fixed CO_2. Our results indicate that WT relies more on the root hair trait for nutrient acquisition (Jungk, 2001), while the enhanced exudation of the hairless *rth3* mutant could aim at compensating the lower absorption surface by increasing nutrient mobility (e.g., via ligand exchange or complexing reactions). Interestingly, *rth3* plants had a higher root diameter than the WT (Table S5) which aligns with the observation from (Vetterlein et al. 2022), and RD was positively correlated to higher exudation rate (Figs. 2b, 3a). This is consistent with the findings of Williams et al. (2022), where the authors found a positive correlation between RD and root exudation of several grassland species.

Exudate characterization showed different exudation patterns in WT compared to *rth3* plants with increasing exudation rates of sugars, amino acids, and phenolics in WT starting from BBCH 59 (Figs. 4, 7) in contrast to the general trend of declining exudation rates with plant development. As reported by Jorda et al. (2022); Vetterlein et al. (2022), WT experienced drought earlier than *rth3* due to higher biomass and stopped growing after BBCH 59. Higher exudation rates of osmoprotectant solutes (i.e., sugars and amino acids) and the increased shoot concentration of K^+ are a clear indication of the mechanism through which WT plants shaped their exudation pattern to face the earlier onset of drought symptoms. Nevertheless, our non-targeted metabolomic results did not show any significant difference in terms of metabolite fingerprinting between the two genotypes. Due to the stronger contribution of plant development in shaping the exudation patterns, our discriminant analysis failed to model significant components when genotype was the investigated factor (Table S7). However, this does not necessarily imply that there are no genotypic differences in the exudation profile. On the contrary, several studies reported intraspecies specific variation in the exudation patterns of maize plants grown under different experimental conditions (Liu et al. 2004; Lopes et al. 2022; Wang et al. 2022). More specifically, in a previous laboratory scale study, Lohse et al. (2023) performed a non-targeted metabolomics comparative study on the same *rth3* and WT maize plants used in this work, showing that a large portion of the detected metabolites had a different or even genotypic-unique regulation.

4.4. Experimental considerations

Most studies in the past have collected root exudates from plants grown in artificial media (i.e., hydroponic, glass beads, percolation) to facilitate exudate collection unaltered by microbial decomposition and/or soil matrix interactions (i.e., sorption of exuded metabolites and primary organic matter soil solution concentrations) (Jones and Darrah, 1993; Kawasaki et al. 2018; Neumann and Römheld 1999; Sasse et al. 2020). However, despite the practicality of artificial systems, plants grown under such conditions are likely to have a different physiology and metabolism than those grown in a natural environment (i.e., soil) (Neumann et al. 2014). Moreover, rhizosphere processes such as root-microbiome interactions and nutrient mobilization, which play a crucial role in shaping exudation, are completely neglected when growing plants in nutrient solution culture. The soil-hydroponic-hybrid exudation sampling approach used in this study is a viable option to obtain ecologically relevant exudation data from the whole root system of field-grown plants if the entire plant, along with its undisturbed root system can be excavated. Despite the drastic shift in environment from soil to solution, root cell contents and therefore also root exudation will still reflect soil conditions if the sampling duration remains short.

5. Conclusion

Results from our study highlight how maize plants can adapt their exudation patterns according to plant phenology and environmental stimuli to support their physiological needs and possibly sustain the successional patterns in the rhizosphere microbiome. We further observed how different growth substrates, as well as the presence or absence of functional root hairs can push the plant to adopt different

foraging strategies, either by enhancing exudation and/or by adapting root morphology. To our knowledge, our study represents the first investigation of maize root exudation throughout the whole plant life cycle under field conditions. Obtaining in-depth knowledge about root exudate quality, C allocation strategies and root plasticity under natural growth conditions is a crucial prerequisite to improve crop yield and to select resilient cultivars and/or root traits to cope with the challenges associated with climate change and the increasing food demand.

Funding

This project was carried out in the framework of the priority programme 2089 "Rhizosphere spatiotemporal organisation - a key to rhizosphere functions" funded by DFG, German Research Foundation (project numbers: 403803214 and 403801423). Eva Oburger was further supported by the ERC Starting Grant 801954 PhytoTrace.

CRediT authorship contribution statement

MS: Investigation, Methodology, Formal analysis, Data curation, Visualization, Writing - original draft. **TSM:** Data curation, Writing - review & editing. **DV:** Conceptualization, Writing - review & editing. **SH:** Resources, Data curation, Writing - review & editing. **EO:** Conceptualization, Methodology, Investigation, Supervision, Funding acquisition, Writing - review & editing. All authors contributed to the article and approved the submitted version.

Declaration of Competing Interest

The authors declare that they have no known competing financial interests or personal relationships that could have influenced the work reported in this paper.

Data Availability

Data will be made available on request.

Acknowledgements

This project was supported by EQ-BOKU VIBT GmbH and the BOKU Core Facility Mass Spectrometry. We would like to thank Caroline Marcon and Frank Hochholdinger (University of Bonn) for providing the maize seeds, Gottfried Wieshammer (Technisches Büro für Bodenkultur, Austria) for construction of columns. From BOKU, we acknowledge Tamas Csakvari for his help with the QTOFMS measurements, Anna Heindl for helping during sampling and WinRHIZO scans, Olivier Duboc for nutrient analyses of plant tissues, Christina Hummel for her help with columns installation at the field site, and Lisa Stein for her help with photometric analyses. From UFZ, we thank Sebastian Häusler, Susanne Schreiter and the UFZ staff from the research station of Bad Lauchstädt for the organizational help, soil columns excavation, and for taking care of the field plot.

Appendix A. Supporting information

Supplementary data associated with this article can be found in the online version at doi:10.1016/j.plantsci.2023.111896.

References

R. Aerts, F.S. Chapin, The mineral nutrition of wild plants revisited: a Re-evaluation of processes and patterns, in: A.H. Fitter, D.G. Raffaelli (Eds.), Advances in Ecological Research, Academic Press, 1999.

E.A. Ainsworth, K.M. Gillespie, Estimation of total phenolic content and other oxidation substrates in plant tissues using Folin–Ciocalteu reagent, Nat. Protoc. 2 (2007) 875–877, https://doi.org/10.1038/nprot.2007.102.

M.S. Aulakh, R. Wassmann, C. Bueno, J. Kreuzwieser, H. Rennenberg, Characterization of root exudates at different growth stages of ten rice (Oryza sativa L.) cultivars, Plant Biol. 3 (2001) 139–148.

D.V. Badri, J.M. Vivanco, Regulation and function of root exudates, Plant, Cell Environ. 32 (2009) 666–681, https://doi.org/10.1111/j.1365-3040.2009.01926.x.

U. Baetz, E. Martinoia, Root exudates: the hidden part of plant defense, Trends Plant Sci. 19 (2014) 90–98, https://doi.org/10.1016/j.tplants.2013.11.006.

H.P. Bais, T.L. Weir, L.G. Perry, S. Gilroy, J.M. Vivanco, The role of root exudates in rhizosphere interactions with plants and other organisms, Annu. Rev. Plant Biol. 57 (2006) 233–266, https://doi.org/10.1146/annurev.arplant.57.032905.105159.

J. Bergmann, A. Weigelt, F. van der Plas, D.C. Laughlin, T.W. Kuyper, N. Guerrero-Ramirez, O.J. Valverde-Barrantes, H. Bruelheide, G.T. Freschet, C.M. Iversen, J. Kattge, M.L. McCormack, I.C. Meier, M.C. Rillig, C. Roumet, M. Semchenko, C. J. Sweeney, J. van Ruijven, L.M. York, L. Mommer, The fungal collaboration gradient dominates the root economics space in plants, Sci. Adv. (2020), https://doi.org/10.1126/sciadv.aba3756.

M.D. Bienert, L.M. Werner, M.A. Wimmer, G.P. Bienert, Root hairs: the villi of plants, Biochem. Soc. Trans. 49 (2021) 1133–1146.

N. Bilyera, C. Hummel, G. Daudin, M. Santangeli, X. Zhang, J. Santner, E. Lippold, S. Schlüter, I. Bertrand, W. Wenzel, S. Spielvogel, D. Vetterlein, B.S. Razavi, E. Oburger, Co-localised phosphorus mobilization processes in the rhizosphere of field-grown maize jointly contribute to plant nutrition, Soil Biol. Biochem. 165 (2022), 108497, https://doi.org/10.1016/j.soilbio.2021.108497.

M. Birouste, E. Zamora-Ledezma, C. Bossard, I.M. Pérez-Ramos, C. Roumet, Measurement of fine root tissue density: a comparison of three methods reveals the potential of root dry matter content, Plant Soil 374 (2014) 299–313, https://doi.org/10.1007/s11104-013-1874-y.

H. Bleiholder, E. Weber, P. Lancashire, C. Feller, L. Buhr, M. Hess, H. Wicke, H. Hack, U. Meier, R. Klose, Growth stages of mono-and dicotyledonous plants, BBCH monograph, Fed. Biol. Res. Cent. Agric. For., Berl. /Braunschw., Ger. (2001) 158.

M.M. Bradford, A rapid and sensitive method for the quantitation of microgram quantities of protein utilizing the principle of protein-dye binding, Anal. Biochem. 72 (1976) 248–254, https://doi.org/10.1016/0003-2697(76)90527-3.

E. Burak, J.N. Quinton, I.C. Dodd, Root hairs are the most important root trait for rhizosheath formation of barley (Hordeum vulgare), maize (Zea mays) and Lotus japonicus (Gifu), Ann. Bot. 128 (2021) 45–57, https://doi.org/10.1093/aob/mcab029.

S. Cadot, H. Guan, M. Bigalke, J.-C. Walser, G. Jander, M. Erb, M.G.A. van der Heijden, K. Schlaeppi, Specific and conserved patterns of microbiota-structuring by maize benzoxazinoids in the field, Microbiome 9 (2021) 103, https://doi.org/10.1186/s40168-021-01049-2.

G. Cai, M.A. Ahmed, The role of root hairs in water uptake: recent advances and future perspectives, J. Exp. Bot. 73 (2022) 3330–3338, https://doi.org/10.1093/jxb/erac114.

A. Canarini, C. Kaiser, A. Merchant, A. Richter, W. Wanek, Root Exudation of Primary Metabolites: Mechanisms and Their Roles in Plant Responses to Environmental Stimuli, Front. Plant Sci. (2019) 10, https://doi.org/10.3389/fpls.2019.00157.

A. Canarini, A. Merchant, F.A. Dijkstra, Drought effects on Helianthus annuus and Glycine max metabolites: from phloem to root exudates, Rhizosphere 2 (2016) 85–97, https://doi.org/10.1016/j.rhisph.2016.06.003.

L.C. Carvalhais, P.G. Dennis, D. Fedoseyenko, M.-R. Hajirezaei, R. Borriss, N. von Wirén, Root exudation of sugars, amino acids, and organic acids by maize as affected by nitrogen, phosphorus, potassium, and iron deficiency, J. Plant Nutr. Soil Sci. 174 (2011) 3–11, https://doi.org/10.1002/jpln.201000085.

J.M. Chaparro, D.V. Badri, M.G. Bakker, A. Sugiyama, D.K. Manter, J.M. Vivanco, Root exudation of phytochemicals in arabidopsis follows specific patterns that are developmentally programmed and correlate with soil microbial functions, PLoS One 8 (2013), e55731, https://doi.org/10.1371/journal.pone.0055731.

J.M. Chaparro, D.V. Badri, J.M. Vivanco, Rhizosphere microbiome assemblage is affected by plant development, ISME J. 8 (2014) 790–803, https://doi.org/10.1038/ismej.2013.196.

R. Chutia, S. Abel, J. Ziegler, Iron and phosphate deficiency regulators concertedly control coumarin profiles in arabidopsis thaliana roots during iron, phosphate, and combined deficiencies, Front. Plant Sci. (2019) 10, https://doi.org/10.3389/fpls.2019.00113.

S. Clemens, M. Weber, The essential role of coumarin secretion for Fe acquisition from alkaline soil, Plant Signal. Behav. 11 (2016), e1114197, https://doi.org/10.1080/15592324.2015.1114197.

C. De-la-Peña, D.V. Badri, Z. Lei, B.S. Watson, M.M. Brandão, M.C. Silva-Filho, L. W. Sumner, J.M. Vivanco, Root secretion of defense-related proteins is development-dependent and correlated with flowering time, J. Biol. Chem. 285 (2010) 30654–30665, https://doi.org/10.1074/jbc.M110.119040.

S. de Weert, H. Vermeiren, I.H.M. Mulders, I. Kuiper, N. Hendrickx, G.V. Bloemberg, J. Vanderleyden, R. De Mot, B.J.J. Lugtenberg, Flagella-driven chemotaxis towards exudate components is an important trait for tomato root colonization by pseudomonas fluorescens, Mol. Plant-Microbe Interactions® 15 (2002) 1173–1180, https://doi.org/10.1094/mpmi.2002.15.11.1173.

Eriksson L., Byrne T., Johansson E., Trygg J., Vikström C. (2013) Multi-and megavariate data analysis basic principles and applications. Umetrics Academy.

Fiehn O. (2002) Metabolomics—the link between genotypes and phenotypes. Functional genomics: 155–171.

H.E. Flores, J.M. Vivanco, V.M. Loyola-Vargas, 'Radicle'biochemistry: the biology of root-specific metabolism, Trends Plant Sci. 4 (1999) 220–226.

T. Galindo-Castañeda, J.P. Lynch, J. Six, M. Hartmann, Improving soil resource uptake by plants through capitalizing on synergies between root architecture and anatomy

and root-associated microorganisms, Front. Plant Sci. (2022) 13, https://doi.org/10.3389/fpls.2022.827369.
B. Galindo-Prieto, L. Eriksson, J. Trygg, Variable influence on projection (VIP) for orthogonal projections to latent structures (OPLS), J. Chemom. 28 (2014) 623–632.
M. Ganther, E. Lippold, M.D. Bienert, M.-L. Bouffaud, M. Bauer, L. Baumann, G. P. Bienert, D. Vetterlein, A. Heintz-Buschart, M.T. Tarkka, Plant age and soil texture rather than the presence of root hairs cause differences in maize resource allocation and root gene expression in the field, Plants 11 (2022) 2883.
A. Gargallo-Garriga, C. Preece, J. Sardans, M. Oravec, O. Urban, J. Peñuelas, Root exudate metabolomes change under drought and show limited capacity for recovery, Sci. Rep. 8 (2018) 1–15.
A. Gransee, L. Wittenmayer, Qualitative and quantitative analysis of water-soluble root exudates in relation to plant species and development, J. Plant Nutr. Soil Sci. 163 (2000) 381–385, https://doi.org/10.1002/1522-2624(200008)163:4<381::AID-JPLN381>3.0.CO;2-7.
J.P. Guyonnet, A.A.M. Cantarel, L. Simon, Haichar FeZ, Root exudation rate as functional trait involved in plant nutrient-use strategy classification, Ecol. Evol. 8 (2018) 8573–8581, https://doi.org/10.1002/ece3.4383.
J. Hansen, I. Møller, Percolation of starch and soluble carbohydrates from plant tissue for quantitative determination with anthrone, Anal. Biochem. 68 (1975) 87–94, https://doi.org/10.1016/0003-2697(75)90682-X.
W.-M. He, Y. Feng, W.M. Ridenour, G.C. Thelen, J.L. Pollock, A. Diaconu, R.M. Callaway, Novel weapons and invasion: biogeographic differences in the competitive effects of Centaurea maculosa and its root exudate (±)-catechin, Oecologia 159 (2009) 803–815.
F. Hochholdinger, T.-J. Wen, R. Zimmermann, P. Chimot-Marolle, O. Da Costa e Silva, W. Bruce, K.R. Lamkey, U. Wienand, P.S. Schnable, The maize (Zea mays L.) roothairless3 gene encodes a putative GPI-anchored, monocot-specific, COBRA-like protein that significantly affects grain yield, Plant J. 54 (2008) 888–898, https://doi.org/10.1111/j.1365-313X.2008.03459.x.
M. Holz, M. Zarebanadkouki, Y. Kuzyakov, J. Pausch, A. Carminati, Root hairs increase rhizosphere extension and carbon input to soil, Ann. Bot. 121 (2017) 61–69, https://doi.org/10.1093/aob/mcx127.
R. Hood-Nowotny, N.H.-N. Umana, E. Inselbacher, P. Oswald- Lachouani, W. Wanek, Alternative methods for measuring inorganic, organic, and total dissolved nitrogen in soil, Soil Sci. Soc. Am. J. 74 (2010) 1018–1027, https://doi.org/10.2136/sssaj2009.0389.
L. Hu, C.A.M. Robert, S. Cadot, X. Zhang, M. Ye, B. Li, D. Manzo, N. Chervet, T. Steinger, M.G.A. van der Heijden, K. Schlaeppi, M. Erb, Root exudate metabolites drive plant-soil feedbacks on growth and defense by shaping the rhizosphere microbiota, Nat. Commun. 9 (2018) 2738, https://doi.org/10.1038/s41467-018-05122-7.
I. Hummel, F. Pantin, R. Sulpice, M. Piques, G. Rolland, M. Dauzat, A. Christophe, M. Pervent, M. Bouteillé, M. Stitt, Y. Gibon, B. Muller, Arabidopsis plants acclimate to water deficit at low cost through changes of carbon usage: an integrated perspective using growth, metabolite, enzyme, and gene expression analysis, Plant Physiol. 154 (2010) 357–372, https://doi.org/10.1104/pp.110.157008.
M.P. Inbaraj, Plant-microbe interactions in alleviating abiotic stress—a mini review, Front. Agron. (2021) 3, https://doi.org/10.3389/fagro.2021.667903.
D.L. Jones, P. Darrah, Re-sorption of organic compounds by roots of Zea mays L. and its consequences in the rhizosphere: II. Experimental and model evidence for simultaneous exudation and re-sorption of soluble C compounds, Plant Soil 153 (1993) 47–59.
D.L. Jones, A. Hodge, Y. Kuzyakov, Plant and mycorrhizal regulation of rhizodeposition, N. Phytol. 163 (2004) 459–480, https://doi.org/10.1111/j.1469-8137.2004.01130.x.
D.L. Jones, A.G. Owen, J.F. Farrar, Simple method to enable the high resolution determination of total free amino acids in soil solutions and soil extracts, Soil Biol. Biochem. 34 (2002) 1893–1902, https://doi.org/10.1016/S0038-0717(02)00203-1.
H. Jorda, M.A. Ahmed, M. Javaux, A. Carminati, P. Duddek, D. Vetterlein, J. Vanderborght, Field scale plant water relation of maize (Zea mays) under drought – impact of root hairs and soil texture, Plant Soil 478 (2022) 59–84, https://doi.org/10.1007/s11104-022-05685-x.
A. Jungk, Root hairs and the acquisition of plant nutrients from soil, J. Plant Nutr. Soil Sci. 164 (2001) 121–129, https://doi.org/10.1002/1522-2624(200104)164:2<121::AID-JPLN121>3.0.CO;2-6.
S. Karlowsky, A. Augusti, J. Ingrisch, M.K.U. Akanda, M. Bahn, G. Gleixner, Drought-induced accumulation of root exudates supports post-drought recovery of microbes in mountain grassland, Front. Plant Sci. 9 (2018) 1593.
A. Kawasaki, S. Okada, C. Zhang, E. Delhaize, U. Mathesius, A.E. Richardson, M. Watt, M. Gilliham, P.R. Ryan, A sterile hydroponic system for characterising root exudates from specific root types and whole-root systems of large crop plants, Plant Methods 14 (2018) 114, https://doi.org/10.1186/s13007-018-0380-x.
P. Kidd, M. Llugany, C. Poschenrieder, B. Gunse, J. Barcelo, The role of root exudates in aluminium resistance and silicon-induced amelioration of aluminium toxicity in three varieties of maize (Zea mays L.), J. Exp. Bot. 52 (2001) 1339–1352.
K.R. Kramer-Walter, P.J. Bellingham, T.R. Millar, R.D. Smissen, S.J. Richardson, D. C. Laughlin, Root traits are multidimensional: specific root length is independent from root tissue density and the plant economic spectrum, J. Ecol. 104 (2016) 1299–1310, https://doi.org/10.1111/1365-2745.12562.
H. Lambers, C. Mougel, B. Jaillard, P. Hinsinger, Plant-microbe-soil interactions in the rhizosphere: an evolutionary perspective, Plant Soil 321 (2009) 83–115, https://doi.org/10.1007/s11104-009-0042-x.
C. Leuschner, D. Hertel, I. Schmid, O. Koch, A. Muhs, D. Hölscher, Stand fine root biomass and fine root morphology in old-growth beech forests as a function of precipitation and soil fertility, Plant Soil 258 (2004) 43–56, https://doi.org/10.1023/B:PLSO.0000016508.20173.80.
C. Leyval, J. Berthelin, Rhizodeposition and net release of soluble organic compounds by pine and beech seedlings inoculated with rhizobacteria and ectomycorrhizal fungi, Biol. Fertil. Soils 15 (1993) 259–267, https://doi.org/10.1007/BF00337210.
Y. Liu, G. Mi, F. Chen, J. Zhang, F. Zhang, Rhizosphere effect and root growth of two maize (Zea mays L.) genotypes with contrasting P efficiency at low P availability, Plant Sci. 167 (2004) 217–223.
M. Lohse, M. Santangeli, T. Steininger-Mairinger, E. Oburger, T. Reemtsma, O. J. Lechtenfeld, S. Hann, The effect of root hairs on exudate composition: a comparative non-targeted metabolomics approach, Anal. Bioanal. Chem. 415 (2023) 823–840, https://doi.org/10.1007/s00216-022-04475-9.
L.D. Lopes, P. Wang, S.L. Futrell, D.P. Schachtman, Sugars and Jasmonic Acid Concentration in Root Exudates Affect Maize Rhizosphere Bacterial Communities, Appl. Environ. Microbiol. 88 (2022) e00971–00922, https://doi.org/10.1128/aem.00971-22.
J.A. Lucas García, C. Barbas, A. Probanza, M.L. Barrientos, F.J. Gutierrez Mañero, Low molecular weight organic acids and fatty acids in root exudates of two Lupinus cultivars at flowering and fruiting stages, Phytochem. Anal. 12 (2001) 305–311, https://doi.org/10.1002/pca.596.
X. Ma, X. Li, U. Ludewig, Arbuscular mycorrhizal colonization outcompetes root hairs in maize under low phosphorus availability, Ann. Bot. 127 (2021) 155–166.
I.C. Meier, P.G. Avis, R.P. Phillips, Fungal communities influence root exudation rates in pine seedlings, FEMS Microbiol. Ecol. 83 (2013) 585–595, https://doi.org/10.1111/1574-6941.12016.
I.C. Meier, T. Tückmantel, J. Heitkötter, K. Müller, S. Preusser, T.J. Wrobel, E. Kandeler, B. Marschner, C. Leuschner, Root exudation of mature beech forests across a nutrient availability gradient: the role of root morphology and fungal activity, N. Phytol. 226 (2020) 583–594, https://doi.org/10.1111/nph.16389.
S.B. Miller, A.L. Heuberger, C.D. Broeckling, C.E. Jahn, Non-Targeted Metabolomics Reveals Sorghum Rhizosphere-Associated Exudates are Influenced by the Belowground Interaction of Substrate and Sorghum Genotype, Int. J. Mol. Sci. 20 (2019) 431.
Y.A. Millet, C.H. Danna, N.K. Clay, W. Songnuan, M.D. Simon, D. Werck-Reichhart, F. M. Ausubel, Innate immune responses activated in Arabidopsis roots by microbe-associated molecular patterns, Plant Cell 22 (2010) 973–990.
S. Mönchgesang, N. Strehmel, S. Schmidt, L. Westphal, F. Taruttis, E. Müller, S. Herklotz, S. Neumann, D. Scheel, Natural variation of root exudates in Arabidopsis thaliana-linking metabolomic and genomic data, Sci. Rep. 6 (2016) 29033, https://doi.org/10.1038/srep29033.
A.L. Neal, S. Ahmad, R. Gordon-Weeks, J. Ton, Benzoxazinoids in Root Exudates of Maize Attract Pseudomonas putida to the Rhizosphere, PLOS ONE 7 (2012), e35498, https://doi.org/10.1371/journal.pone.0035498.
G. Neumann, S. Bott, M. Ohler, H.-P. Mock, R. Lippmann, R. Grosch, K. Smalla, Root exudation and root development of lettuce (Lactuca sativa L. cv. Tizian) as affected by different soils, Front. Microbiol. (2014) 5, https://doi.org/10.3389/fmicb.2014.00002.
G. Neumann, V. Römheld, Root excretion of carboxylic acids and protons in phosphorus-deficient plants, Plant Soil 211 (1999) 121–130, https://doi.org/10.1023/A:1004380832118.
E. Oburger, B. Gruber, Y. Schindlegger, W.D.C. Schenkeveld, S. Hann, S.M. Kraemer, W. W. Wenzel, M. Puschenreiter, Root exudation of phytosiderophores from soil-grown wheat, New Phytol. 203 (2014) 1161–1174, https://doi.org/10.1111/nph.12868.
E. Oburger, D.L. Jones, Sampling root exudates – Mission impossible, Rhizosphere 6 (2018) 116–133, https://doi.org/10.1016/j.rhisph.2018.06.004.
E. Oburger, H. Schmidt, C. Staudinger, Harnessing belowground processes for sustainable intensification of agricultural systems, Plant Soil 478 (2022a) 177–209, https://doi.org/10.1007/s11104-022-05508-z.
E. Oburger, C. Staudinger, A. Spiridon, V. Benyr, D. Aleksza, W. Wenzel, M. Santangeli, A quick and simple spectrophotometric method to determine total carbon concentrations in root exudate samples of grass species, Plant Soil (2022b), https://doi.org/10.1007/s11104-022-05519-w.
Ostonen I., Püttsepp Ü., Biel C., Alberton O., Bakker M.R., Lõhmus K., Majdi H., Metcalfe D., Olsthoorn A.F.M., Pronk A., Vanguelova E., Weih M., Brunner I. (2007) Specific root length as an indicator of environmental change. Plant Biosystems - An International Journal Dealing with all Aspects of Plant Biology 141: 426–442. doi: 10.1080/11263500701626069.
H.A. Pantigoso, J. Yuan, Y. He, Q. Guo, C. Vollmer, J.M. Vivanco, Role of root exudates on assimilation of phosphorus in young and old Arabidopsis thaliana plants, PLoS One 15 (2020), e0234216, https://doi.org/10.1371/journal.pone.0234216.
P. Pétriacq, A. Williams, A. Cotton, A.E. McFarlane, S.A. Rolfe, J. Ton, Metabolite profiling of non-sterile rhizosphere soil, Plant J. 92 (2017) 147–162, https://doi.org/10.1111/tpj.13639.
L. Philippot, S. Hallin, G. Börjesson, E.M. Baggs, Biochemical cycling in the rhizosphere having an impact on global change, Plant Soil 321 (2009) 61–81, https://doi.org/10.1007/s11104-008-9796-9.
C. Preece, J. Peñuelas, Rhizodeposition under drought and consequences for soil communities and ecosystem resilience, Plant Soil 409 (2016) 1–17, https://doi.org/10.1007/s11104-016-3090-z.
S. Ray, S. Mishra, K. Bisen, S. Singh, B.K. Sarma, H.B. Singh, Modulation in phenolic root exudate profile of Abelmoschus esculentus expressing activation of defense pathway, Microbiol. Res. 207 (2018) 100–107, https://doi.org/10.1016/j.micres.2017.11.011.
T. Rongsawat, J.-B. Peltier, J.-C. Boyer, A.-A. Véry, H. Sentenac, Looking for root hairs to overcome poor soils, Trends Plant Sci. 26 (2021) 83–94.
T. Rosenkranz, E. Oburger, M. Baune, G. Weber, M. Puschenreiter, Root exudation of coumarins from soil-grown Arabidopsis thaliana in response to iron deficiency, Rhizosphere 17 (2021), 100296, https://doi.org/10.1016/j.rhisph.2020.100296.

T. Rudrappa, K.J. Czymmek, P.W. Paré, H.P. Bais, Root-secreted malic acid recruits beneficial soil bacteria, Plant Physiol. 148 (2008) 1547–1556, https://doi.org/10.1104/pp.108.127613.
P. Ryser, The mysterious root length, Plant Soil 286 (2006) 1–6.
P. Ryser, H. Lambers, Root and leaf attributes accounting for the performance of fast- and slow-growing grasses at different nutrient supply, Plant Soil 170 (1995) 251–265, https://doi.org/10.1007/BF00010478.
J. Sasse, S.M. Kosina, M. de Raad, J.S. Jordan, K. Whiting, K. Zhalnina, T.R. Northen, Root morphology and exudate availability are shaped by particle size and chemistry in Brachypodium distachyon, Plant Direct 4 (2020), e00207, https://doi.org/10.1002/pld3.207.
E.L. Schymanski, J. Jeon, R. Gulde, K. Fenner, M. Ruff, H.P. Singer, J. Hollender, Identifying small molecules via high resolution mass spectrometry: communicating confidence, Environ. Sci. Technol. 48 (2014) 2097–2098, https://doi.org/10.1021/es5002105.
V.A. Seitz, B.B. McGivern, R.A. Daly, J.M. Chaparro, M.A. Borton, A.M. Sheflin, S. Kresovich, L. Shields, M.E. Schipanski, K.C. Wrighton, J.E. Prenni, Variation in root exudate composition influences soil microbiome membership and function, Appl. Environ. Microbiol. 88 (2022), e0022622, https://doi.org/10.1128/aem.00226-22.
V.L. Singleton, J.A. Rossi, Colorimetry of total phenolics with phosphomolybdic-phosphotungstic acid reagents, Am. J. Enol. Vitic. 16 (1965) 144–158.
S. Sinha Roy, B. Mittra, S. Sharma, T.K. Das, C.R. Babu, Detection of root mucilage using an anti-fucose antibody, Ann. Bot. 89 (2002) 293–299, https://doi.org/10.1093/aob/mcf040.
S. Steinkellner, V. Lendzemo, I. Langer, P. Schweiger, T. Khaosaad, J.-P. Toussaint, H. Vierheilig, Flavonoids and strigolactones in root exudates as signals in symbiotic and pathogenic plant-fungus interactions, Molecules 12 (2007) 1290–1306.
I.A. Stringlis, R. de Jonge, C.M.J. Pieterse, The age of coumarins in plant–microbe interactions, Plant Cell Physiol. 60 (2019) 1405–1419, https://doi.org/10.1093/pcp/pcz076.
Stringlis I.A., Yu K., Feussner K., de Jonge R., Van Bentum S., Van Verk M.C., Berendsen R.L., Bakker P.A.H.M., Feussner I., Pieterse C.M.J. (2018) MYB72-dependent coumarin exudation shapes root microbiome assembly to promote plant health. Proceedings of the National Academy of Sciences 115: E5213-E5222. doi:⟨doi:10.1073/pnas.1722335115⟩.
L. Sun, M. Ataka, M. Han, Y. Han, D. Gan, T. Xu, Y. Guo, B. Zhu, Root exudation as a major competitive fine-root functional trait of 18 coexisting species in a subtropical forest, New Phytol. 229 (2021) 259–271, https://doi.org/10.1111/nph.16865.
R. Tiziani, B. Miras-Moreno, A. Malacrinò, R. Vescio, L. Lucini, T. Mimmo, S. Cesco, A. Sorgonà, Drought, heat, and their combination impact the root exudation patterns and rhizosphere microbiome in maize roots, Environ. Exp. Bot. 203 (2022), 105071, https://doi.org/10.1016/j.envexpbot.2022.105071.
N.M. van Dam, H.J. Bouwmeester, Metabolomics in the rhizosphere: tapping into belowground chemical communication, Trends Plant Sci. 21 (2016) 256–265.
D. Vetterlein, E. Lippold, S. Schreiter, M. Phalempin, T. Fahrenkampf, F. Hochholdinger, C. Marcon, M. Tarkka, E. Oburger, M. Ahmed, M. Javaux, S. Schlüter, Experimental platforms for the investigation of spatiotemporal patterns in the rhizosphere—Laboratory and field scale, J. Plant Nutr. Soil Sci. 184 (2021) 35–50, https://doi.org/10.1002/jpln.202000079.
D. Vetterlein, M. Phalempin, E. Lippold, S. Schlüter, S. Schreiter, M.A. Ahmed, A. Carminati, P. Duddek, H. Jorda, G.P. Bienert, M.D. Bienert, M. Tarkka, M. Ganther, E. Oburger, M. Santangeli, M. Javaux, J. Vanderborght, Root hairs matter at field scale for maize shoot growth and nutrient uptake, but root trait plasticity is primarily triggered by texture and drought, Plant Soil 478 (2022) 119–141, https://doi.org/10.1007/s11104-022-05434-0.
V. Vives-Peris, A. Gómez-Cadenas, R.M. Pérez-Clemente, Citrus plants exude proline and phytohormones under abiotic stress conditions, Plant Cell Rep. 36 (2017) 1971–1984.
P. Wang, L.D. Lopes, M.G. Lopez-Guerrero, K. van Dijk, S. Alvarez, J.-J. Riethoven, D. P. Schachtman, Natural variation in root exudation of GABA and DIMBOA impacts the maize root endosphere and rhizosphere microbiomes, J. Exp. Bot. 73 (2022) 5052–5066, https://doi.org/10.1093/jxb/erac202.
Y. Wang, Y. Cai, Y. Cao, J. Liu, Aluminum-activated root malate and citrate exudation is independent of NIP1;2-facilitated root-cell-wall aluminum removal in Arabidopsis, Plant Signal Behav. 13 (2018), e1422469, https://doi.org/10.1080/15592324.2017.1422469.
Y. Wang, W. Ren, Y. Li, Y. Xu, Y. Teng, P. Christie, Y. Luo, Nontargeted metabolomic analysis to unravel the impact of di (2-ethylhexyl) phthalate stress on root exudates of alfalfa (Medicago sativa), Sci. Total Environ. 646 (2019) 212–219, https://doi.org/10.1016/j.scitotenv.2018.07.247.
A. Weinhold, S. Döll, M. Liu, A. Schedl, Y. Pöschl, X. Xu, S. Neumann, N.M. van Dam, Tree species richness differentially affects the chemical composition of leaves, roots and root exudates in four subtropical tree species, J. Ecol. 110 (2022) 97–116, https://doi.org/10.1111/1365-2745.13777.
C.E. Wells, D.M. Eissenstat, Beyond the roots of young seedlings: the influence of age and order on fine root physiology, J. Plant Growth Regul. 21 (2002) 324–334, https://doi.org/10.1007/s00344-003-0011-1.
T.-J. Wen, P.S. Schnable, Analyses of mutants of three genes that influence root hair development in Zea mays (Gramineae) suggest that root hairs are dispensable, Am. J. Bot. 81 (1994) 833–842, https://doi.org/10.1002/j.1537-2197.1994.tb15564.x.
L.A. Weston, U. Mathesius, Root exudation: the role of secondary metabolites, their localisation in roots and transport into the rhizosphere, in: A. Morte, A. Varma (Eds.), Root Engineering: Basic and Applied Concepts, Springer Berlin Heidelberg, Berlin, Heidelberg, 2014.
A. Williams, F.T. de Vries, Plant root exudation under drought: implications for ecosystem functioning, in: New Phytol, 225, 2020, pp. 1899–1905, https://doi.org/10.1111/nph.16223.
A. Williams, H. Langridge, A.L. Straathof, H. Muhamadali, K.A. Hollywood, R. Goodacre, F.T. de Vries, Root functional traits explain root exudation rate and composition across a range of grassland species, J. Ecol. 110 (2022) 21–33, https://doi.org/10.1111/1365-2745.13630.
J. Yuan, J. Zhao, T. Wen, M. Zhao, R. Li, P. Goossens, Q. Huang, Y. Bai, J.M. Vivanco, G. A. Kowalchuk, R.L. Berendsen, Q. Shen, Root exudates drive the soil-borne legacy of aboveground pathogen infection, Microbiome 6 (2018) 156, https://doi.org/10.1186/s40168-018-0537-x.
K. Zhalnina, K.B. Louie, Z. Hao, N. Mansoori, U.N. da Rocha, S. Shi, H. Cho, U. Karaoz, D. Loqué, B.P. Bowen, M.K. Firestone, T.R. Northen, E.L. Brodie, Dynamic root exudate chemistry and microbial substrate preferences drive patterns in rhizosphere microbial community assembly, Nat. Microbiol. 3 (2018) 470–480, https://doi.org/10.1038/s41564-018-0129-3.
M. Zhao, J. Zhao, J. Yuan, L. Hale, T. Wen, Q. Huang, J.M. Vivanco, J. Zhou, G. A. Kowalchuk, Q. Shen, Root exudates drive soil-microbe-nutrient feedbacks in response to plant growth. Plant, Cell Environ. 44 (2021) 613–628, https://doi.org/10.1111/pce.13928.
J. Ziegler, S. Schmidt, R. Chutia, J. Müller, C. Böttcher, N. Strehmel, D. Scheel, S. Abel, Non-targeted profiling of semi-polar metabolites in Arabidopsis root exudates uncovers a role for coumarin secretion and lignification during the local response to phosphate limitation, J. Exp. Bot. 67 (2015) 1421–1432, https://doi.org/10.1093/jxb/erv539.

Web references

Mass Bank of North America. Available at: ⟨https://mona.fiehnlab.ucdavis.edu/⟩ (Accessed: March 2023).
METLIN. Available at: ⟨https://metlin.scripps.edu/⟩ (Accessed: August 2022).